Elsevier Editorial System(tm) for Science of the Total Environment

Manuscript Draft

Manuscript Number: STOTEN-D-17-05347

Title: Developing strategies to reduce spray drift in pneumatic spraying in vineyards: assessment of the parameters affecting droplet size in pneumatic spraying

Article Type: Research Paper

Keywords: pneumatic spraying; droplet size; spray drift; spray technology; droplet homogeneity

Corresponding Author: Dr. Antonio Miranda-Fuentes, Ph.D.

Corresponding Author's Institution: University of Córdoba

First Author: Antonio Miranda-Fuentes, Ph.D.

Order of Authors: Antonio Miranda-Fuentes, Ph.D.; Paolo Marucco; Emilio J González-Sánchez; Emilio Gil; Marco Grella; Paolo Balsari

Abstract: Pneumatic sprayers are widely used in vineyards due to their very fine droplet size, which, on the other hand, makes the drift risk to become an important problem to be considered. The aim of this study was to assess the effect of the spout diameter on the spray droplet size and uniformity achieved for different liquid flow rates (LFR) and air flow rates (AFR).
A test bench was developed to simulate a real pneumatic sprayer under laboratory conditions, and it was empirically adjusted to match the air pressure conditions as closely as possible to real working conditions. Two positions of insertion of the liquid hose, the conventional position (CP) and an alternative position (AP), were tested for three LFRs, 1.00, 1.64, and 2.67 L min-1, and four AFRs, 0.280, 0.312, 0.345, and 0.376 m3 s-1. The air speed decrease between the two insertion points of the liquid hose was measured. A Malvern SprayTec® instrument was used to measure the droplet size, and the D50, D10, and D90 parameter values were obtained. The relative SPAN factor (RSF) was also calculated. A model to predict variations in D50 was fitted using the aforementioned parameters. The results show that a change in the diameter of the spout significantly changes the droplet size, producing a mean increase of 59.45% in D50 and similar increases in D10 and D90. The model developed to predict variations in D50 has a very high degree of accuracy (R2 = 0.945). The relative decrease in the air speed along the spout is constant, with a mean value of 8.35%. The results of the study show that the droplet size produced in pneumatic spraying can be modified easily by varying the air spout dimensions. This should be taken into account by manufacturers from a design point of view.

Suggested Reviewers: Joao Paulo A Rodrigues da Cunha
Universidade Federal de Uberlândia
jpcunha@iciag.ufu.br

Gianfranco Pergher

*Graphical Abstract

PNEUMATIC SPRAYER

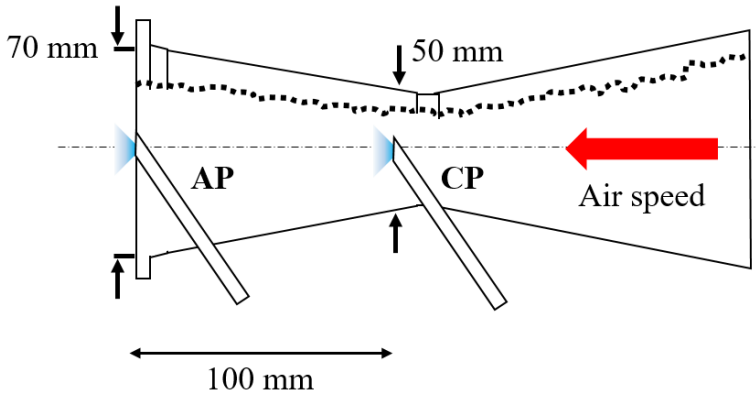

PNEUMATIC DROPLETS GENERATION –SPOUT–

Droplet spectra measurements using laser spray diffraction system.

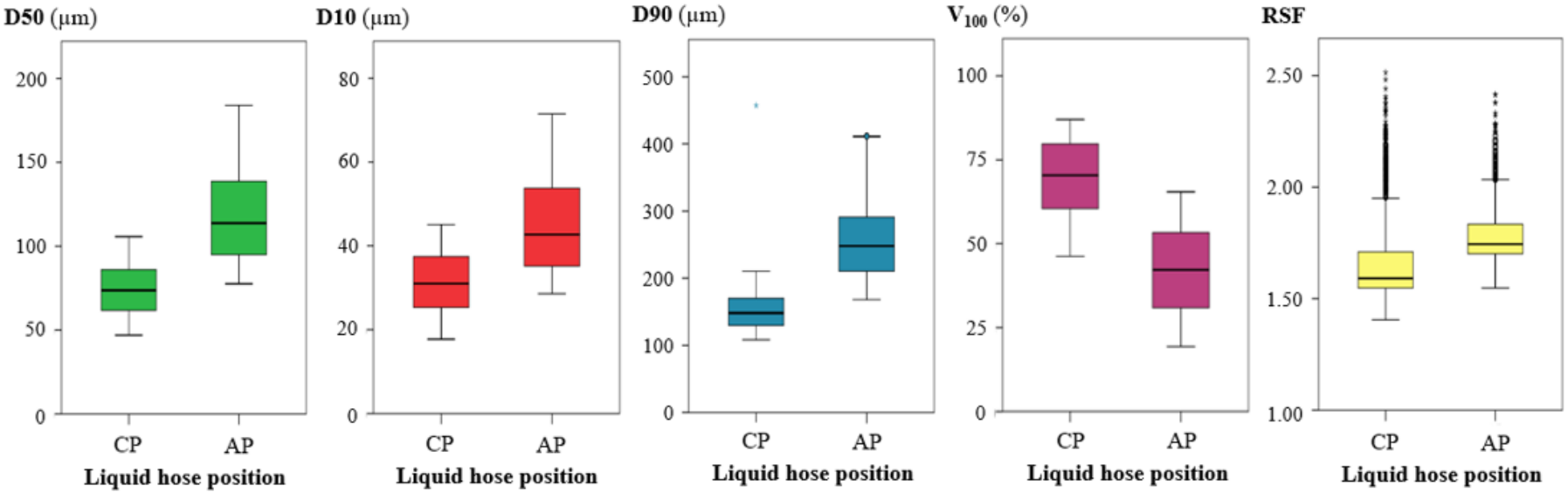

HIGHLIGHTS

- Pneumatic sprayers produce very fine droplets that are very likely to be drifted.
- Pneumatic nozzle's air spout diameter had a strong influence on the droplet size.
- Airflow rate and liquid flow rate are strongly related to droplet size.
- Droplet size can be accurately predicted with the aforementioned parameters.
- Drift risk can be reduced by modifying the spout characteristics.

Developing strategies to reduce spray drift in pneumatic spraying in vineyards: assessment of the parameters affecting droplet size in pneumatic spraying

Miranda-Fuentes, A.[a,*], Marucco, P.[b], González-Sánchez, E. J.[a], Gil, E.[c], Grella, M.[b], Balsari, P.[b]

[a] Department of Rural Engineering, University of Córdoba, Ctra. Nacional IV, km 396, Campus de Rabanales, Córdoba 14014, Spain.

[b] Department of Agricultural, Forest and Food Sciences (DiSAFA), University of Turin (UNITO), Largo Paolo Braccini 2, 10095 Grugliasco (TO), Italy.

[c] Department of Agri Food Engineering and Biotechnology (DEAB), Universitat Politècnica de Catalunya (UPC), Esteve Terradas 8, Campus del Baix Llobregat D4, 08860 Castelledfels, Barcelona, Spain.

* Corresponding author: Antonio Miranda-Fuentes. E-mail address: antonio.miranda@uco.es. Telephone: +34 957 212 689

Abstract

Pneumatic sprayers are widely used in vineyards due to their very fine droplet size, which, on the other hand, makes the drift risk to become an important problem to be considered. The aim of this study was to assess the effect of the spout diameter on the spray droplet size and uniformity achieved for different liquid flow rates (LFR) and air flow rates (AFR).

A test bench was developed to simulate a real pneumatic sprayer under laboratory conditions, and it was empirically adjusted to match the air pressure conditions as

closely as possible to real working conditions. Two positions of insertion of the liquid hose, the conventional position (CP) and an alternative position (AP), were tested for three LFRs, 1.00, 1.64, and 2.67 L min^{-1}, and four AFRs, 0.280, 0.312, 0.345, and 0.376 m^3 s^{-1}. The air speed decrease between the two insertion points of the liquid hose was measured. A Malvern SprayTec® instrument was used to measure the droplet size, and the D50, D10, and D90 parameter values were obtained. The relative SPAN factor (RSF) was also calculated. A model to predict variations in D50 was fitted using the aforementioned parameters.

The results show that a change in the diameter of the spout significantly changes the droplet size, producing a mean increase of 59.45% in D50 and similar increases in D10 and D90. The model developed to predict variations in D50 has a very high degree of accuracy (R^2 = 0.945). The relative decrease in the air speed along the spout is constant, with a mean value of 8.35%. The results of the study show that the droplet size produced in pneumatic spraying can be modified easily by varying the air spout dimensions. This should be taken into account by manufacturers from a design point of view.

Keywords: pneumatic spraying, droplet size, spray drift, spray technology, droplet homogeneity.

1. Introduction

Plant protection product (PPP) applications have improved substantially in recent years due to the new European legal framework, beginning with the European Directive for Sustainable Use of Pesticides 2009/128/EC (EC, 2009), which focuses on increasing spray application efficiency, supporting strategies for integrated control, and spray dose

reduction. This new paradigm has its origin in concern about the various factors that contribute to the risk of PPP pollution, which is related mainly to field run-off and spray drift (TOPPS-Prowadis, 2014).

This risk is attracting increased attention from the general population and, of course, from the scientific community. This social concern is justified by the fact that spray drift affects not only water pollution and the environment but also adjacent sensitive areas, such as schools and natural parks, and also bystanders (Butler Ellis et al., 2014).

According to ISO22866:2005 (ISO, 2005), drift is defined as 'the quantity of plant protection product that is carried out of the sprayed area (treated) by the action of air currents during the application process'. In any orchard, this includes droplets that move horizontally through the orchard canopy and beyond the orchard, as well as droplets that move upward above the canopy (via direct spraying into the air or upward diffusion from the sprayed canopy). For this reason, spray drift generated during spray applications to bush/tree crops is complex and difficult to control (Delele et al., 2007; Llorens et al., 2016; van de Zande et al., 2008). Some authors have quantified that, during an orchard spray application, 30 to 50% of the total applied PPP spray mixture can be lost to the air from the targeted site to a non-target receptor site (Van den Berg et al., 1999). In addition to the more localised movement of agrochemical residues in turbulent air masses downwind of the application, residues can also become concentrated in inversions or stable air masses and be transported long distances (Felsot et al., 2011). Thus, during and immediately after spray application, non-target receptors, including water (Dabrowski et al., 2003), plants (Marrs et al., 1993), and animals (Davis et al., 1990; Ernst et al., 1991; Lahr et al., 2000) can be acutely exposed and may therefore face the risk of adverse effects. Thus, drift may cause damage to non-target plants, contaminate water courses, generate illegal residues in food and feed

commodities (Benbrook & Baker, 2014), and cause adverse exposure to animals and humans (Felsot et al., 2011; Butler Ellis et al., 2010).

According to Hofman and Solseng (2001) the factors affecting pesticide emissions to the air during the application process can be divided into technical and environmental factors.

Among the technical factors that affect spray drift, the size of the particles has a large impact on the off-target drift (Take et al., 1996), as this parameter has been found to be more important than the environmental wind speed during the spray drift generation process (Bird et al., 1996; Combellack, 1982; Frost & Ware, 1970; Grella et al., 2017). Thus, producing a fine spray tends to increase the drift risk (Bode et al., 1976). Likewise, in bush/tree crop spray applications, the air flow of the sprayer's fan plays a crucial role in ensuring the biological efficacy of treatments and reducing the drift risk. Correct adjustment of the air jet for the canopy size, leaf density, and row distance reduces spray drift by increasing spray deposition (Dekeyser et al., 2014; Doruchowski et al., 2002; Duga et al., 2015; Marucco et al., 2008).

Thus, for many years, the main efforts to prevent spray drift have been focused on generating larger droplets. Nozzle type (Nuyttens et al., 2007a) and nozzle size (Guler et al., 2007) have the greatest effects on droplet size and velocity spectra. With hydraulic nozzles, the main strategy for reducing spray drift is the use of air induction (AI) nozzles (Felsot et al., 2011; TOPPS-Prowadis, 2014), which have been proven to reduce spray drift substantially, compared to conventional nozzles, by maintaining similar deposition values (Derksen et al., 2007; Ganzelmeier & Rautmann, 2000) and thus ensuring consistency in the biological efficacy of treatments (Doruchowski et al., 2017; Garcerá et al., 2017).

100 Among the various parameters used in characterising the range of droplet sizes in a
101 spray, the most commonly used is the volumetric median diameter (VMD or D50). Other
102 useful parameters include the tenth- and ninetieth-percentile diameters (D10 and D90)
103 and the percentage of the volume composed of droplets with diameters less than 100
104 μm (V_{100}). In characterising the relationship between spray drift and droplet size, many
105 researchers have considered droplets smaller than 75 μm (Hobson et al., 1990; Hobson
106 et al., 1993; Miller and Hadfield, 1989), 100 μm (Bode, 1984; Byass and Lake, 1977; Gil
107 et al., 2014; Grover et al., 1978), 150 μm (Combellack et al., 1996; Yates et al., 1985), or
108 200 μm (Bouse et al., 1990) to be the ones most prone to drift. Zhu et al. (1994) found
109 that spray particles less than 50 μm in diameter remain suspended in the air indefinitely
110 or until they evaporate. Although there is no specific droplet size range that is likely to
111 drift under all conditions, droplets with diameters less than 100 μm are generally
112 accepted to be highly driftable. The V_{100} parameter is therefore often used as an
113 indicator of the drift risk potential associated with a nozzle or application technology
114 (van de Zande et al., 2008). Many authors have found significant relationships between
115 drift and V_{100} (Arvidsson et al., 2011; Baetens et al., 2008; Bode, 1984; Bouse et al.,
116 1990; Combellack et al., 1996; Gil et al., 2015; Nuyttens et al., 2007a; 2010; 2011).
117 Pneumatic sprayers are very popular and are widely used in the most important
118 vineyard areas all around the world. Their suitability for low to very low volume
119 application rates, the large working capacity of the sprayers, and the importance of
120 generating good and uniform coverage together with precise penetration into the
121 canopy make this type of spray technology an interesting option, mainly for large farms.
122 Pneumatic sprayers represent approximately 25% of the total market for sprayers for
123 bush/tree crops, with very widespread use in vineyards in southern Europe. However,

few advances have been made in this technology with respect to the droplet size and the collateral risk of drift.

The pneumatic diffusers that are typically mounted on vineyard sprayers consist of spouts in which spray droplets are generated by the action of a high-speed, high-pressure air stream on a liquid conveyed at low pressure (maximum of 0.15 MPa) inside the spout (Balsari & Scienza, 2003). The Venturi effect created at the internal part of the spouts generates very fine droplets. Although there have been very few studies of droplet size spectra produced by pneumatic sprayers (Balsari et al., 2016), the diameters of the droplets are known to be typically less than 100 μm, which is the threshold below which droplets become very driftable. This driftability increases when droplets are blown away by pneumatic cannons mounted on the top part of the sprayer. These cannons disperse the spray to nearby rows with high air speeds and flight distances, which increases the time during which the spray is exposed to wind and consequently increases the drift risk.

With hydraulic nozzles, the main factors affecting the characteristics of the droplet spectra are the nozzle type and size, and the working pressure. In contrast, with pneumatic sprayer spouts, the main parameters affecting the droplet size spectra are the variations in the air speed and liquid flow rate, which depend on the physical characteristics of the spouts and the characteristics of the elements that release the liquid into the air stream, including their positions inside the spouts. The air flow speed is inversely correlated to the droplet size: higher air speeds produce finer droplets. The opposite is true of the relation between the droplet size and the liquid flow rate: higher liquid flow rates produce larger droplets (Márquez, 2007). However, there is little reliable information available about the quantitative relations between these two parameters and droplet size.

149 The main objective of this work was to assess quantitatively the influence of the
150 working parameters, i.e., the air flow rate and liquid flow rate, on the size of the droplets
151 generated in a pneumatic cannon similar to the ones commonly used in vineyard
152 sprayers. Another objective was to assess the influence of the spout diameter at the
153 release point of the liquid on the droplet size. Droplet uniformity and its relationship to
154 the risk of drift during vineyard spraying using pneumatic sprayers were also examined
155 in this study.
156

157 ## 2. Materials and methods

Abbreviations

AFR → Air flow rate

AP → Alternative insertion position of the liquid hose in the pneumatic nozzle

CP → Conventional insertion position of the liquid hose in the pneumatic nozzle

D10 → Diameter for which a volume fraction of 10 percent is made up of drops with diameters smaller than this this value (expressed in μm)

D50 → Volume median diameter of diameter for which a volume fraction of 50 percent is made up of drops with diameters smaller than this this value (expressed in μm)

D90 → Diameter for which a volume fraction of 90 percent is made up of drops with diameters smaller than this this value (expressed in μm)

HP → Hose position of the liquid hose in the pneumatic nozzle

LFR → Liquid flow rate in the spraying circuit

RSF → Relative SPAN factor, a measure of the droplet homogeneity in the spray population

SD → Spout diameter of the pneumatic nozzle

V_{100} → Portion of the sprayed volume composed of droplets finer than 100 μm.

VMD → Volumetric mean diameter, equivalent to D50

158

159 *2.1. Test bench setup*

160 Trials were carried out in the laboratory of the Department of Agricultural, Forest, and
161 Food Sciences (DiSAFA) of the University of Torino (Grugliasco, Torino, Italy). A
162 prototype of a test bench was mounted using three different spaces (Fig. 1).

163

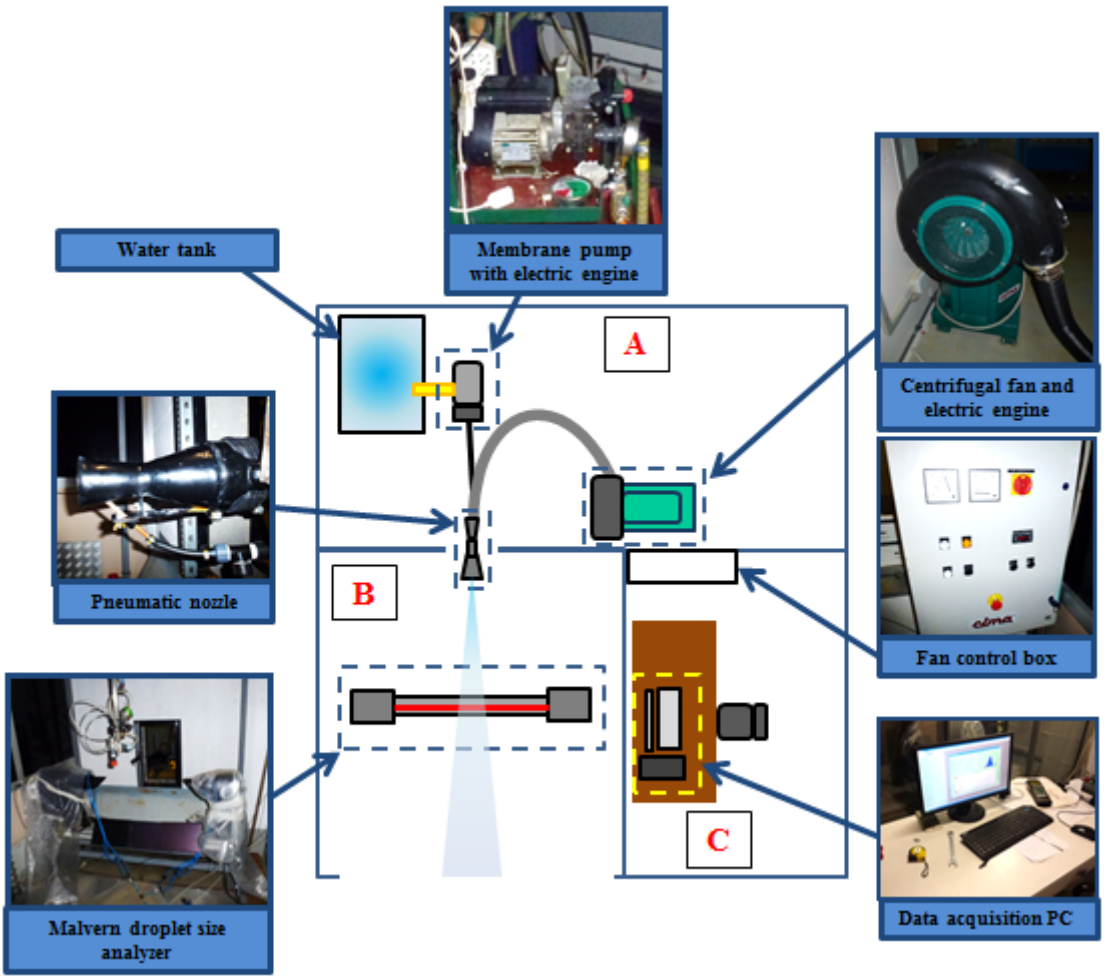

164

165 Figure 1. Laboratory setup for the test bench and difference spaces: A. Spraying
166 equipment, B. Spray droplet measurement instruments, and C. Trial control and data
167 acquisition elements.

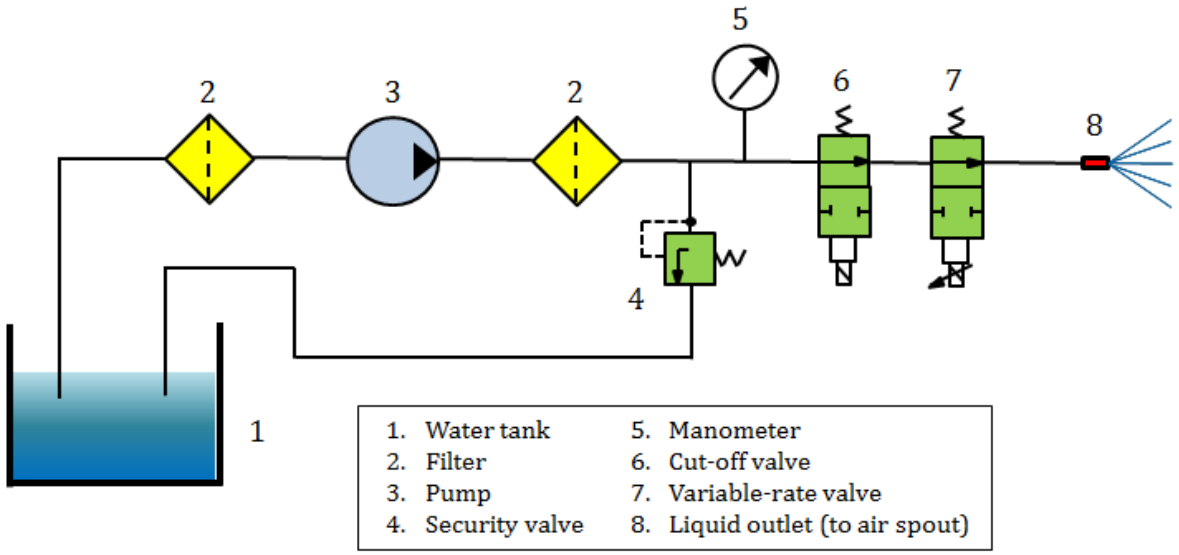

Figure 2. Spraying circuit used in the test bench.

The test bench was mounted using three different spaces, i.e., three different rooms, to separate the spraying elements (A in Fig. 1) from the measurement area (B in Fig. 1) and from the data acquisition and analysis area (C in Fig. 1). Spaces A and B were connected through a window through which the air spout was placed.

The spraying circuit (Fig. 2) was powered by a membrane pump (AR 202, Annovi Reverberi S.P.A., Modena, Italy), with a maximum pressure of 2.0 MPa and a maximum flow rate of 23.2 L min^{-1}. A manometer with a measurement resolution of ± 0.01 MPa) was used to adjust the working pressure and thereby control the liquid flow rate (Fig. 2). The pump was driven by an asynchronous 230-V, 15.3-A electrical engine (model 100 L_2, Ravel Srl, Bomporto, Italy) and fed by a water tank with a 50-L capacity.

The pneumatic system consisted of a centrifugal fan (CIMA SpA, Pavia, Italy) controlled by a 230-V, 15.9-A electrical engine (LEX-LEN 200 L-8, Euromotori Srl, Macherio, Italy) and a flexible tube 2.5 m in length and 150 mm in diameter that conducted the air towards the air spout. The fan rotary speed was remotely controlled using a dial positioned in the fan control box (Fig. 1). This control device allowed for a working

186 resolution of ± 1 rpm. The actual fan rotary speed was checked using an optical
187 tachometer (Photo tachometer, Lutron Electronic Enterprise Co, Ltd., Taipei, Taiwan).
188
189 *2.2. Pneumatic nozzle description*
190 To assess the effect of the spout diameter on the size of the generated droplets, two
191 insertion positions for the liquid hose (hose positions, HP) were tested: the conventional
192 position (CP) and an alternative position (AP) (Fig. 3), corresponding to spout diameters
193 of 50 mm and 70 mm, respectively. Because the AP location was farther from the air
194 flow inlet than the CP, a reduction in the air speed (AS) was expected for a constant air
195 flow rate. Consequently, as the droplet diameter is inversely proportional to the air
196 speed in pneumatic spraying (Di Prinzio et al., 2010), a decrease in the AS was expected
197 when using this AP. The resulting droplet sizes produced for the two positions were
198 determined using a commercial pneumatic nozzle (model TC.SAV2C, CIMA SpA, Pavia,
199 Italy) of the type that is usually mounted on the top part of a vineyard pneumatic
200 sprayer to spray adjacent rows.

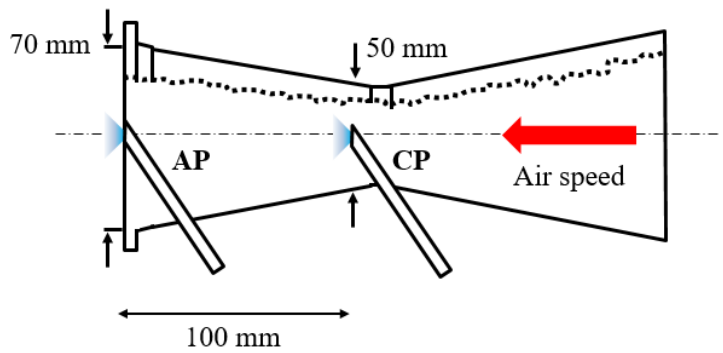

201
202 Figure 3. Conventional (CP) and alternative (AP) positions of insertion of the liquid hose
203 in the air spout.
204

Alongside the holes made in the spout to insert the liquid hose, a curved implement was inserted into the spout to measure the pressure along the longitudinal axis and perpendicular to the air current lines.

2.3. Adjustment of the fan rotary speed to match the air pressure to real conditions

The stationary fan was calibrated using a real pneumatic sprayer (model TC.SAV2C, CIMA SpA, Pavia, Italy) equipped with two upper outlets (cannons) (spray-head model Savoy, CIMA SpA). The sprayer was attached to a tractor (T4, New Holland Inc, Torino, Italy). The calibration procedure consisted of determining the relationship between the rotary speeds of the test bench's fan and the real sprayer's fan to maintain similar working conditions. The purpose of this was to ensure that the air pressures measured at a specific point in the air spout would be the same in both cases.

The air pressure in the sprayer's spout was measured at a point on its mid plane (Fig. 4a). An implement was used to measure the air flow pressure at the centre of the spout and in the direction of the air speed vector, and a manometer with a measurement resolution of ± 1 mm H_20) was used to measure, in terms of water height, the air pressure of the sprayer when its fan was rotating at 300, 350, 400, 450, 500, and 550 rpm. The fan rotation speeds were measured with an optical tachometer (Photo tachometer, Lutron Electronic Enterprise Co, Ltd.).

The measurements performed using the test bench's fan and the sprayer's fan were taken using the same procedures and sampling positions (Fig. 4b). In addition, the same fan rotary speeds used in the real sprayer were measured.

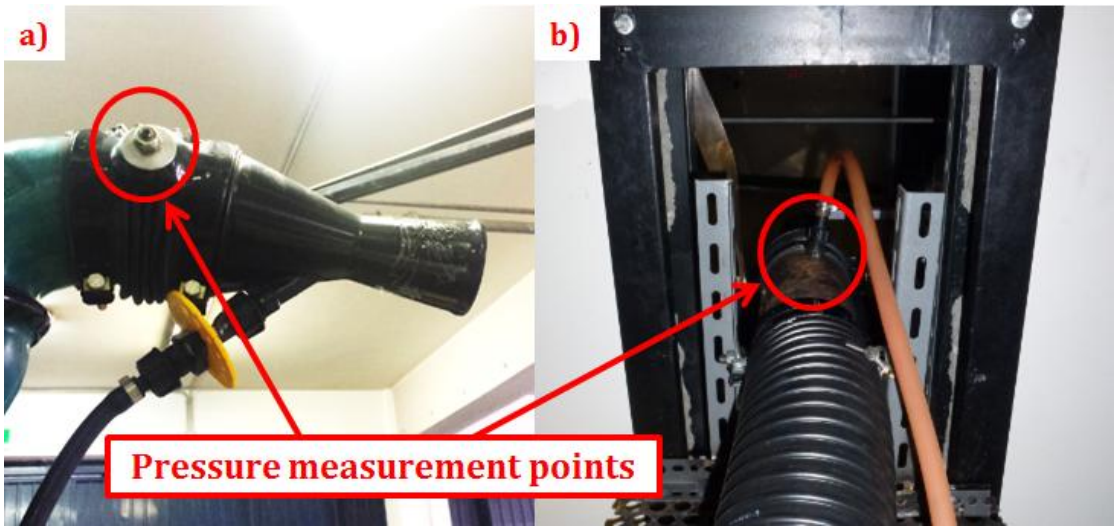

Figure 4. Air pressure sampling position in: a) the real sprayer, and b) the prototype.

Once the relationship between fan rotary speed and air pressure was obtained, the operating speed of the test bench fan was calculated according to the regression curve for each fan rotary speed tested (Figure 7). The air pressure measurements were repeated at the calculated speed values and empirically corrected to be equal to those obtained for the sprayer fan for the corresponding fan rotary speed values. This ensured that the pressure was exactly the same in both systems.

2.4. Air speed reduction along the spout longitudinal axis

The variation in the air speed along the longitudinal axis of the spout was checked and found to be proportional to the air flow rate. The air speed values were measured along the longitudinal axis of the spout between the two intended positions of insertion of the liquid hose. The starting position was coincident with the original insertion point of the liquid hose (CP), and the final point was coincident with the air spout outlet (AP).

The air speeds were measured with a Pitot-tube-based anemometer (Testo 400, Testo Inc, Lenzkirch, Germany) with a measurement resolution of ± 0.01 hPa, a differential pressure of 1.28 m s^{-1}, and a measurement range of up to +2000 hPa (571.43 m s^{-1}).

247 Speeds were measured at a frequency of 1 Hz over a time period of 20 s, and the average
248 value was automatically calculated by the device.
249 An implement was developed and fixed to the air spout to position the Pitot tube
250 precisely in the centre of the spout (Fig. 5). The two extreme positions and the central
251 one were tested.

252
253 Figure 5. Implement for measuring the air speed in the centre of the air spout.
254
255 A series of eight air flow rates (AFRs) (those generated by the fan at 350, 400, 450, 500,
256 550, 600, 650, and 700 rpm) were tested. The four calibrated rotary speed
257 corresponding to 350, 400, 450, and 550 rpm were also tested using the conventional
258 pneumatic sprayer. Three replicates, each obtained over a 20-s acquisition period of
259 time, were performed for each air flow rate tested.
260
261 *2.5. Droplet size measurement*
262 The droplet sizes produced were measured using a Malvern Spraytec® laser diffraction
263 system (STP5342, Malvern Instruments Ltd., Worcestershire, UK) (Fig. 6). The
264 instrument has a maximum measurement frequency of 10 kHz and a measurement
265 range of 0 to 2000 μm. As pneumatic sprayers generate very small droplets, a 300-mm

lens was used. The instrument includes software (SprayTec Software v3.30, Malvern) for managing the data acquisition and charting.

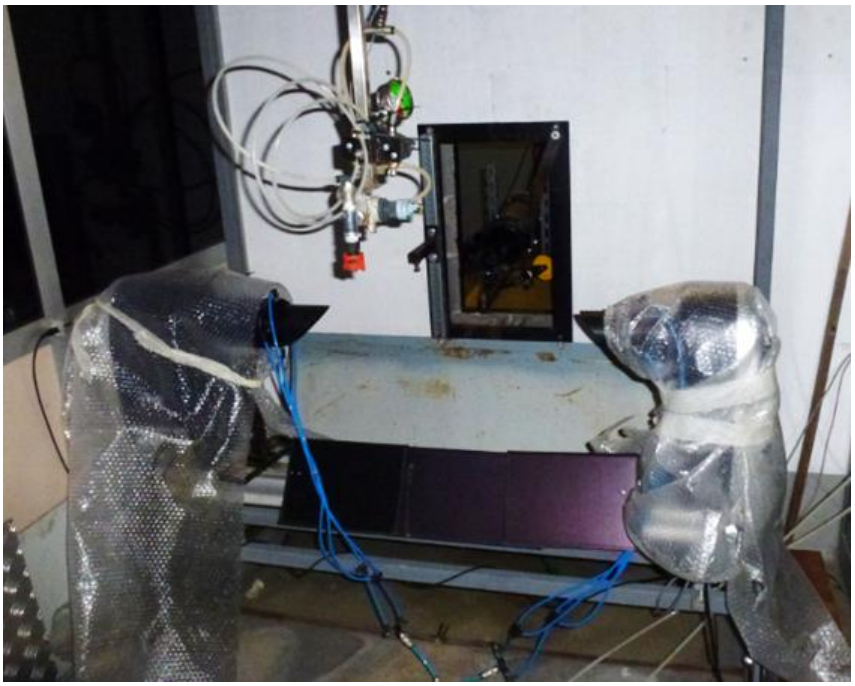

Figure 6. Malvern SprayTec® droplet size analyser.

The laser device was placed inside the designated chamber (B - Fig. 1) to avoid possible disturbance to the air flow and thus to the measurement process. An air current was used to prevent the coalescence of droplets on the surface of the lens cover. The instrument was covered properly to protect it from the spray liquid. All of the tests were conducted with the nozzle positioned orthogonally at a distance of 50 cm from the laser beam emitted by the instrument. This distance was adjusted in previous tests to ensure that representative droplet sizes were obtained.

The data were acquired for 60 s at a 1-Hz frequency. The 10^{th} percentile diameter (D10), 50^{th} percentile or volumetric median diameter (D50), 90th-percentile diameter (D90), and percentage volume composed of droplets finer than 100 μm in diameter (V_{100}) were determined for each configuration tested. The frequencies of a series of pre-established

droplet size intervals, distributed on a logarithmic scale, were also measured. Three replications were carried out for each configuration. A replication was considered to be complete when 60 values had been obtained for each combination of parameters.

2.6. Experimental design

The experiment was designed to consider two different hose positions (HP) were tested (CP and AP, Fig. 3), three liquid flow rate (LFR) levels, and four air flow rate (AFR) levels (Table 1). The LFR and AFR levels used are shown in Table 1.

For each configuration of the aforementioned parameters, D10, D50, D90, V_{100}, and the SPAN factor (RSF, which reflects the droplet uniformity) were measured or calculated. The RSF calculation is expressed in Equation 1.

$$RSF = \frac{D90 - D10}{D50} \quad [1]$$

The experimental design was a completely randomised factorial and three replications for each configuration. A total of 24 different combinations (Table 1) of the HP (two positions), LFR (three levels), and AFR (four levels) were tested. When the measurements for all of the air flow rate levels had been obtained, one replication of the trial was considered to have been completed. This cycle was repeated three times.

Table 1. Studied variables with adjustable parameters and selected levels for each one.

Studied parameter	**Air spout diameter** (SD)	**Liquid flow rate** (LFR)	**Air flow rate** (AFR)
Studied levels	50/70 mm	1.00/1.64/2.67 L min^{-1}	0.280/0.312/0.348/0.376 $m^3 s^{-1}$
Regulation based on	Position of the liquid hose	Position of the regulatory disc	Rotary speed of the fan
Positions tested	Conventional/Alternative	Positions 3/5/7	541/598/663/720 rpm

306 The values chosen for the different parameters (Table 1) were selected according to the
307 specifications of the manufacturer and the working ranges commonly used by farmers
308 in the area. The spraying liquid pressure was kept constant at 0.1 MPa.
309
310 *2.7. Statistical data analysis*
311 An analysis of covariance (ANCOVA, α = 0.05) was conducted to detect differences in air
312 speed reduction along the longitudinal axis of the spout for the different AFR levels,
313 using the distance to the original position as a covariate. Normality and homocedasticity
314 were assessed using Shapiro-Wilk and Levène tests (α = 0.05), respectively.
315 Differences in droplet size were assess using the R-software to import all of the
316 individual data files into a general matrix. A preliminary analysis was performed using
317 this software to plot the results and perform a Shapiro-Wilk test (α = 0.05) of the
318 normality of the data and a Levène test (α = 0.05) of the homogeneity of the variances.
319 The matrix with all of the data was then exported for statistical analysis. SPSS v20 (IBM,
320 Armonk, NY, USA) was used to perform the analysis of variance (ANOVA) and develop
321 the linear model.
322 A three-way ANOVA was performed to assess the influences of the different test
323 parameters on the droplet size parameters and the droplet uniformity. In addition, the
324 significance of the effects of interactions between the factors was checked.
325 Linear regression models were obtained to express the effects of the liquid and air flow
326 rates on the calculated D50 and RSF values for both the CP and AP. A linear model
327 (Equation 2) was fitted to predict VMD as a function of LFR and AFR.
328

$$D50 = \beta_0 + \beta_1 \times SD + \beta_2 \times LFR + \beta_3 \times AFR + \varepsilon$$

329 [2]

In this equation, β_0 is the constant term of the regression corresponding to the D50 value when the predictive parameters are zero; β_1, β_2, and β_3 are the magnitudes of the effects of SD, LFR and AFR, respectively, on D50; and ε is the residual error of the model. Prior to the model development, the normality and homoescedasticity of the residuals were checked (Hair et al., 2009).

3. Results and discussion

3.1. Adjustment of the test bench to simulate a real sprayer

Figure 7 show the air pressure values for the commercial sprayer and the spraying prototype.

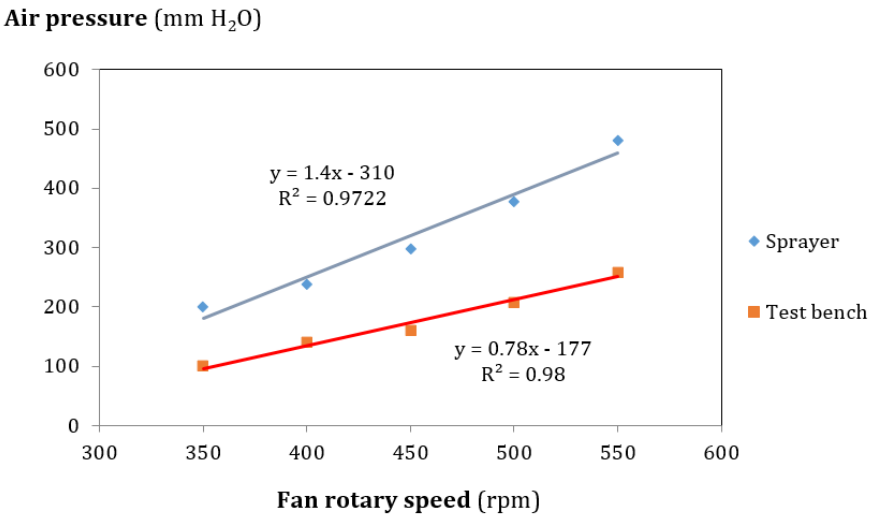

Figure 7. Air pressure versus rotary speed for the sprayer and the test bench.

Figure 7 shows that the air pressure is directly correlated to the air flow rate in both systems. Nevertheless, the prototype generated a lower air pressure than the commercial equipment. The fan air flow pressure values for the test bench were almost

half those of the sprayer over the entire range of fan rotary speeds investigated, as indicated by the slope of the regression line (1.8004). The measured values were very consistent, with no significant differences in the air pressure detected among the different replications of the measurements (coefficient of variation CV < 5%). This has remarkable practical importance, as the test bench can be configured easily to match any rotary speed of the real sprayer. This makes it possible to produce target air flow rates for droplet size measurements (Table 1). The results of the manual adjustment are shown in Table 2, along with the corresponding rotary speed values of the real sprayer and the calculated theoretical values.

Table 2. Results of the adjustment of the rotary speed values to make the pressure match in both systems.

Parameter		**Values**			
Sprayer rotary speed	(rpm)	350	400	450	500
Measured pressure	(mm_{H2O})	180	240	300	380
Calculated test bench rotary speed	(rpm)	462	552	642	732
Adjusted test bench rotary speed	(rpm)	541	598	663	720

Differences were detected between the calculated and adjusted rotary speed values. These differences may have been due to errors in the adjustment of the rotary speed of the prototype by the control box and the adjustment of the rotary speed of the sprayer's fan with the optical tachometer.

3.2. Air speed reduction along the spout longitudinal axis

The air speed reductions for the three measured positions along the spout's longitudinal axis for the different air flow rates are shown in Figure 8 and Table 3.

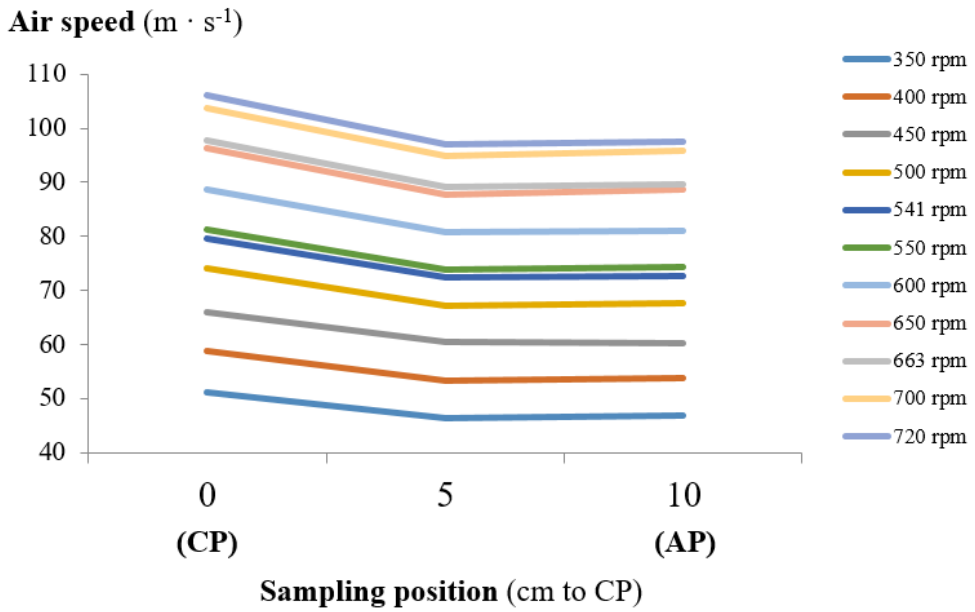

372

373 Figure 8. Air speed values along the longitudinal axis of the air spout.

374

375 The ANCOVA revealed significant differences ($p = 0.0349$) in the speed decreases
376 associated with the different air flow rates. This indicates that AFR significantly affects
377 the air speed change along the spout and thus the absolute difference in air speed
378 between the two liquid hose insertion positions. Table 3 shows the absolute and relative
379 air speed drops between sampling points 0 and 10.

380

381 Table 3. Mean air speeds for sampling positions 0, 5, and 10 along the longitudinal axis
382 of the air spout and absolute and relative air speed drops.

	Air speed (m s^{-1})				
Prototype	Sampling position			Δspeed	Δspeed
rpm	0	5	10	(m s^{-1})	(%)
350	51.80	46.51	46.84	4.23	8.29
400	58.83	53.44	53.85	4.98	8.47
450	65.90	60.54	60.30	5.60	8.50
500	74.10	67.16	67.75	6.35	8.57
541	79.51	72.39	72.76	6.74	8.48
550	81.36	73.81	74.36	6.99	8.60
600	88.58	80.69	81.02	7.56	8.53
650	96.31	87.68	88.56	7.75	8.04
663	97.70	89.26	89.60	8.11	8.30
700	103.78	94.92	95.76	8.02	7.73
				Mean	8.35
				SD	0.28
				CV (%)	3.31

As Table 3 shows, there was a constant relative air speed drop along the spout, with a CV among the measured values of 3.31%. This means that for any value of the air flow rate, a constant air speed drop should be expected, and therefore, a change in the insertion point of the spout will have the same effect for a constant speed decrease. This is logical, considering that the AFR is calculated as the air speed multiplied by the cross-sectional area of the spout. Therefore, the higher the AFR is, the higher the absolute speed drop will be, while the percentage decrease remains the same. This is important because it can be confirmed that the working principle of the droplet size change works under real measured conditions and consequently can be applied to check the differences.

3.3. Droplet size

397 The results of the ANOVA for all of the dependent variables revealed that every test
398 parameter considered and their interactions (double and triple) were highly significant
399 in all cases for D50, D10, D90, V100, and RSF ($p < 10^{-4}$ in every case).
400
401 The droplet size parameters D50, D10, and D90, along with V_{100} and RSF for both
402 positions of the liquid hose, for all possible combinations of cases, are shown in Figure 9.
403 The differences in the parameters are clearly evident for both parameters and thus
404 confirm the ANOVA results. The high variability observed for each parameter is the
405 result of the inclusion of all of the combinations and the presentation together of very
406 different results.
407
408

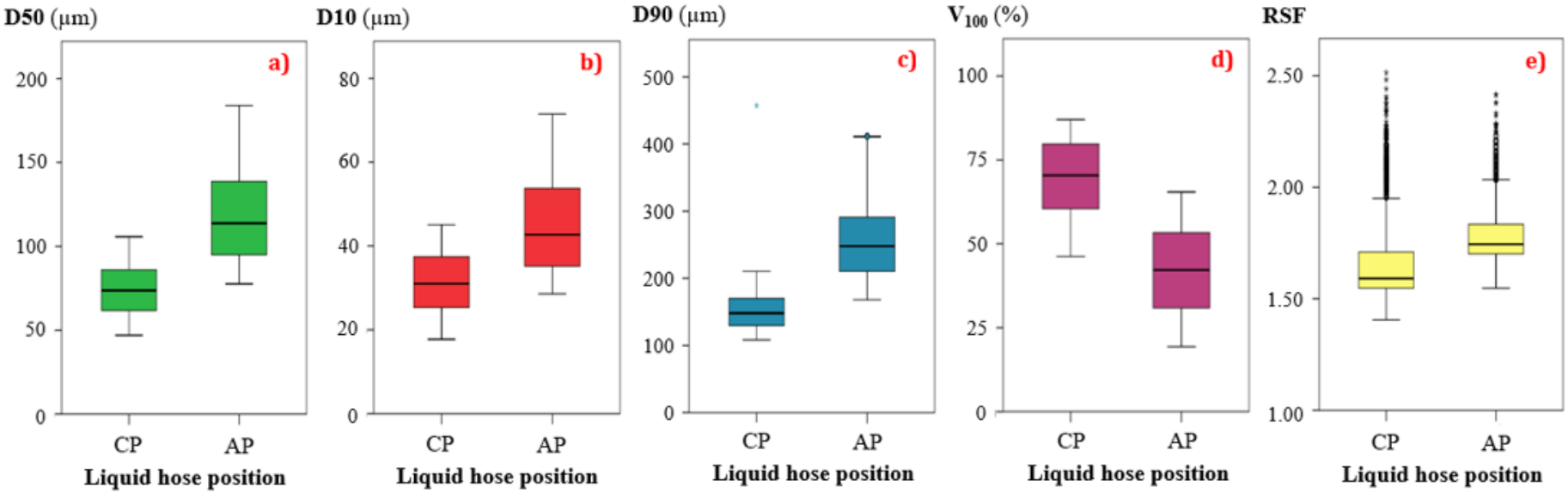

Figure 9. Boxplots for the variables D50 (a), D10 (b), D90 (c), V_{100} (d), and RSF (e). The boxplots include all of the combinations of AFR and LFR considered.

418

As Figure 9 shows, D50, D10, and D90 were considerably higher for the AP in all cases, as was the variability in the results. In the particular case of D50, the median value rose from 74.25 µm to 118.39 µm. This is a 59.45% mean increase in the D50 parameter between the two tested positions, reflecting larger droplet sizes overall. According to the ASAE S-572 droplet size classification (Southcombe et al., 1997), which is used to assess the spray drift of droplets of different sizes, the use of the AP can the droplet sizes from the very fine (VF) category to the fine (F) category, the limit between the two being 100 μm.

The AP also increased the median values of the D10 and D90 parameters, from 31.19 μm to 45.28 µm and from 151.92 µm to 254.82 µm, respectively. These are increases of 45.17% for D10 and 67.73% for D90. Note that the increases in the median values are proportional to the droplet sizes, with the minimum and maximum increases corresponding to the D10 and D90 parameters, respectively.

The D50 mean values (µm) for each combination and the standard errors for each position of the liquid hose are shown in Figure 10.

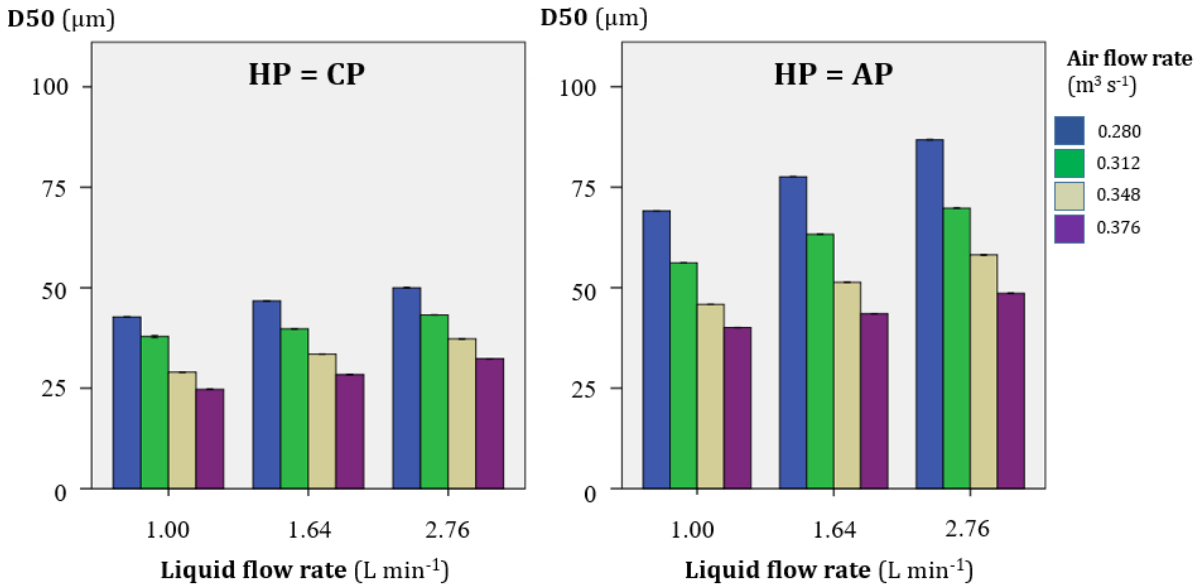

436 Figure 10. D50 values for different combinations of variables for the two positions of the
437 liquid hose. The error bars indicate the standard errors.
438
439 The values were very stable, with a very small standard error for each combination.
440 Given that each bar reflects 180 values, this indicates that the instrument was very
441 accurate in measuring the droplet size and that the values obtained are highly reliable.
442 For both positions of the liquid hose, D50 increases with LFR and decreases with AFR.
443 These results are consistent with the results obtained by Manhani et al. (2013), who
444 found that an increase in the air flow rate produced a decrease in the VMD. These results
445 are also consistent with the findings of Di Prinzio et al. (2010), who reported that the
446 droplet size achieved in pneumatic spraying can be changed by changing the ratio
447 between the liquid and air flow rates.
448 The mean values for the inner position of the liquid hose were below the 100 μm, with
449 the maximum mean value for the highest LFR corresponding to the lowest AFR (D50 =
450 99.99 μm) and the minimum mean value for the lowest LFR corresponding to the
451 highest AFR (D50 = 49.46 μm). The effect of LFR in this case is not very remarkable,
452 resulting in a mean VMD increase of 23.56% from the minimum to the maximum AFR.
453 The values for the AP of the liquid hose were, in general, greater than or equal to 100
454 μm, except for the highest AFR values at the lowest LFR positions. With this
455 configuration, the maximum D50 was obtained with the highest LFR and the lowest AFR
456 and occurred with the CP (D50 = 173.61 μm). The minimum value was obtained in the
457 opposite case (D50 = 80.12 μm). An increase in droplet size is very important because it
458 is the most important parameter affecting spray drift (Combellack, 1982; Grella et al.,
459 2017), with droplets smaller than 100 μm very likely to drift as a result of wind action
460 (van De Zande et al., 2008).

The VMD values for the AP of the liquid hose were higher than those for the CP for all combinations of the test parameters. A mean D50 increase of 58.62% was obtained using AP. Figure 11 shows the mean relative differences in D50 between the two liquid hose positions for the different combinations of AFR and LFR.

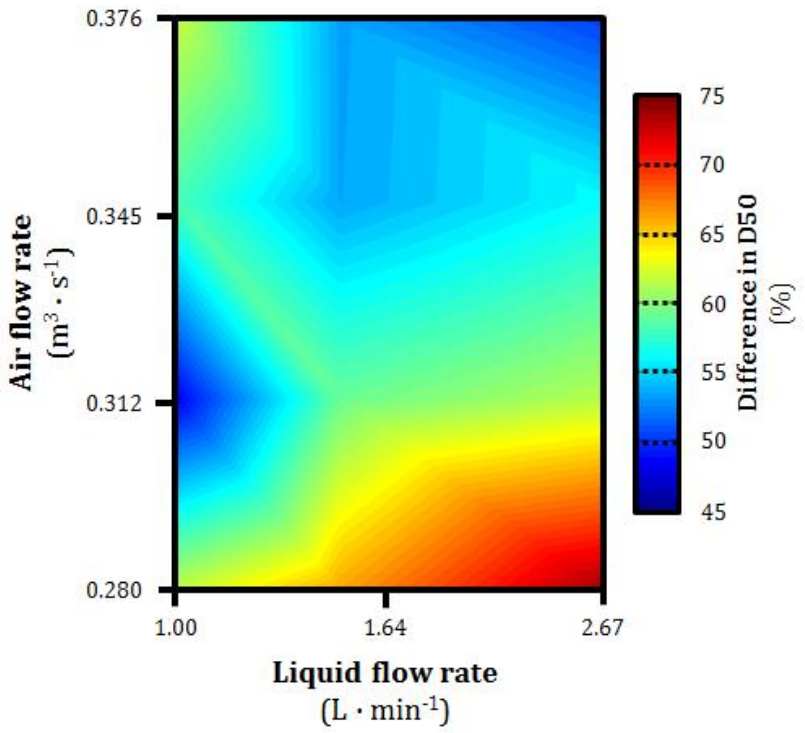

Figure 11. Mean relative differences in D50 between the two liquid hose positions for every combination of AFR and LFR.

The mean relative differences ranged from 48.29% to 73.63%, and as Figure 11 shows, there was not a clear trend in the differences. The largest differences are concentrated in the lower right-hand corner of the graph, which corresponds to the highest LFR and the lowest AFR. This combination produces the coarsest droplets for both positions, which means that the largest differences arise under the most favourable conditions for producing larger droplets. However, the smallest differences are not concentrated in the opposite corner of the graph, which means that the differences remains constant up to a

point for the combination of both parameters, beyond which point it increases. This finding could be important in terms of recommendations given to farmers and applicators concerning how to maximise differences in droplet size.

A linear model was developed to predict D50 as a function of SD, LFR and AFR (Eq. 3).

$$D50 = 121.145 + 2.207 \times SD + 11.900 \times LFR - 543.460 \times AFR \quad [3]$$

In this equation, D50 is expressed in μm, SD in mm, LFR in L min^{-1}, and AFR in m^3 s^{-1}.

All the variables considered were found to be highly significant ($p < 10^{-4}$), and the model has a coefficient of determination $R^2 = 0.945$. This means that the three variables explain most of the differences observed in D50 and that the behaviour of the tested spout can be almost completely explained by these parameters. Note that SD coefficient in this equation is 2.2, which means that a small increase in SD can produce a large increase in D50. This can also be seen by comparing the relative air speed difference along the spout (Table 3) and the relative increase in the droplet diameter (Fig. 11). The mean air speed decrease was 8.35%, and the mean D50 increase was greater than 50%. This is a very important finding because it shows that the air spout diameter at the point of spray generation can be varied to vary the droplet size generated. Design criteria that reflect this fact can be provided by sprayer manufacturers to help farmers reduce the drift risk in their applications, especially when spraying at long distances from the target canopy, where this risk is higher.

3.4. Droplet driftability

Droplet driftability is significantly related to the V_{100} parameter (Hilz and Vermeer, 2013; Nuyttens et al., 2007b; van de Zande et al., 2008). The V_{100} results for every combination of the independent variables considered in this study are shown in Figure 12.

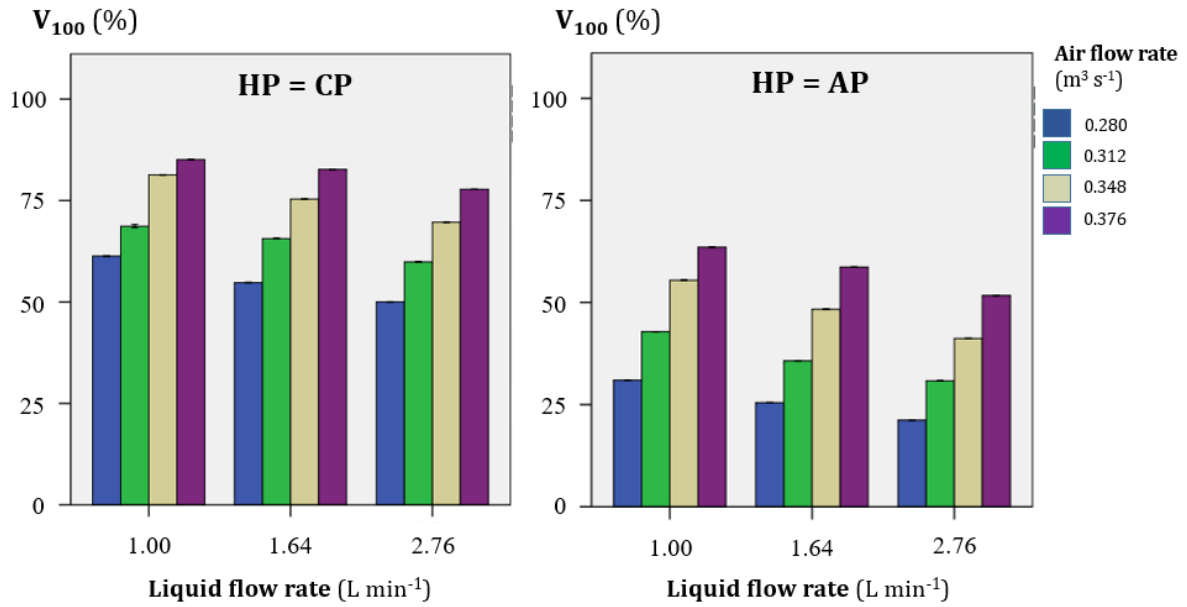

Figure 12. V_{100} for different combinations of variables for the two positions of the liquid hose. The error bars indicate the standard errors.

The high V_{100} values obtained for the CP represent a very high drift risk, as these two parameters are positively correlated (Gil et al., 2014). With this HP, most mean values are above 50%, and some configurations lead to mean values of nearly 90%. A comparison of this top value with one obtained using a conventional hollow-cone nozzle (V_{100} value of 23.1% for an Albuz ATR Lilac) and used as a reference by other authors (van de Zande et al., 2008) shows that use of the pneumatic cannon increases the value of this parameter by a factor of nearly four (an increase of 390%). On the other hand, for the AP, the V_{100} values were significantly reduced to below 75% in every case. It is also noteworthy that it is possible to have, in the most favourable case, V_{100} values of 24%, which are similar to those obtained with the aforementioned reference nozzle.

517 Pneumatic spraying is known to produce very fine droplets, but for the AP of the liquid
518 hose and the lowest AFR, the driftable spray fraction is similar to that obtained with a
519 hydraulic nozzle. This finding has useful implications for high wind speed conditions
520 and for cases in which it is absolutely necessary to continue a spraying process even in
521 adverse conditions. Nevertheless, a mean reduction of 27.18% in V_{100} can be achieved
522 just by modifying the hose position in the cannon. This reduction would be associated
523 with a drift risk reduction of 60.80% according to the formula for spray drift reduction
524 potential based on V_{100} proposed by van de Zande et al. (2008), in which the reference
525 V_{100} value is the mean of the values obtained with the CP. This reduction is similar to
526 some reductions achieved using low-drift nozzles rather than conventional hollow-cone
527 nozzles, according to these authors.
528
529 *3.5. Droplet spectra uniformity*
530 Significant differences in the droplet spectra uniformity, as measured by the RSF, were
531 detected for all of the studied variables and their interactions ($p < 10^{-4}$ in every case).
532 This means that the hose AP does not achieve the uniformity of the CP, and therefore,
533 the new configuration alters the uniformity of the droplet population. This occurs
534 because of the influence of the studied variables on the D10 and D90 parameters. As
535 Figure 9 shows, the percentage increase was higher for D90 and, therefore, the range in
536 the spray volume between these two limits is higher for the AP of the liquid hose.
537 Nevertheless, and as Figure 13 shows, the RSF increase was much smaller than the
538 increases in the droplet size parameters, with an absolute increase of 0.124% from the
539 median value of 1.654% obtained with the CP to 1.778% for the AP. This corresponds to
540 a relative increase of 7.50%.

Figure 13 shows the mean RSF values obtained for every combination of AFR and LFR considered for the two positions of the liquid hose.

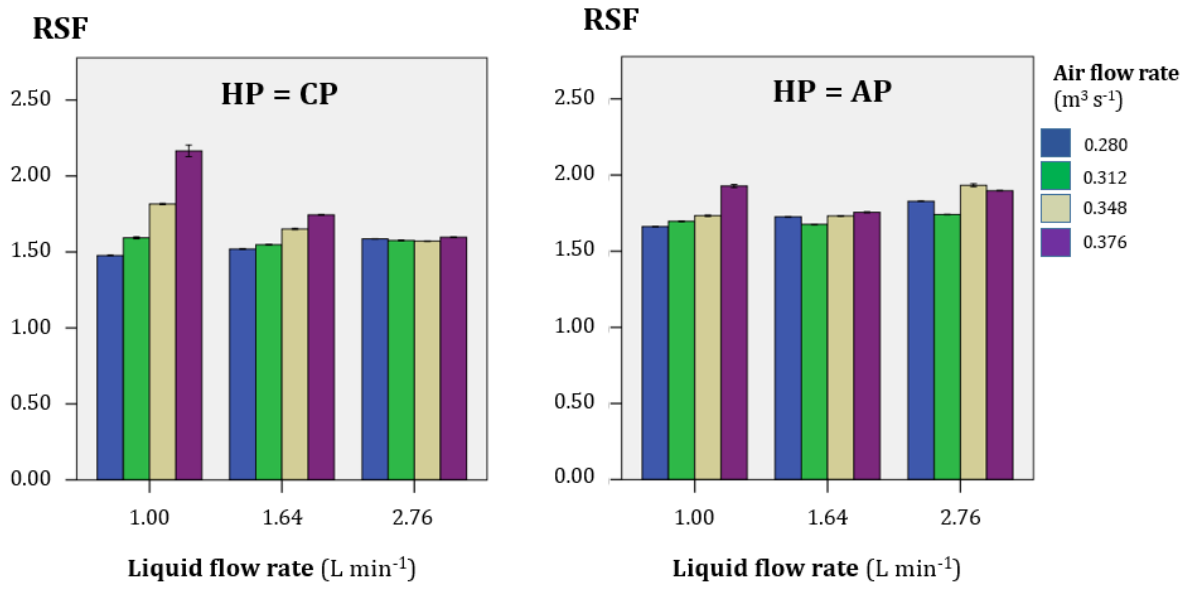

Figure 13. Mean relative SPAN factor (RSF) for every tested combination of LFR and AFR for the two tested positions of the liquid hose. The error bars indicate the standard errors.

The variation in RSF within each combination was still low, even with the errors associated with the three measured parameters combined. The differences in RSF did not seem to follow any particular trend with respect to the LFR or AFR values and was very stable except for the lowest LFR and the CP of the liquid hose. However, the ANOVA test revealed that significant differences existed ($p < 10^{-4}$) for each parameter and their interaction. A Tukey test ($\alpha = 0.05$) detected three homogeneous groups corresponding to the three tested LFRs, with mean values of 1.7588% for an LFR of 1.00 L min^{-1} (position 3 of the regulatory disc), 1.7162% for an LFR of 2.67 L min^{-1} (position 7), and 1.6691% for an LFR of 1.64 L min^{-1} (position 5). These results indicate that RSF did not increase with LFR; rather, RSF was lowest for the intermediate LFR value. Nevertheless,

558 the relative differences were very low, so an important influence on the spray was not
559 expected.
560 Three homogeneous groups corresponding to the tested AFRs were detected using a
561 Tukey test, and RSF was found to increase with increasing AFR. The mean RSF results
562 for AFR levels of 0.280 $m^3 s^{-1}$ and 0.312 $m^3 s^{-1}$ (541 rpm and 598 rpm of the fan) were
563 not significantly different (1.6330% and 1.6385%, respectively). Differences were
564 detected between these two groups and each of the others, and between the other two,
565 with mean values of 1.7394% for the AFR of 0.348 $m^3 s^{-1}$ (663 rpm) and 1.8480% for the
566 AFR of 0.376 $m^3 s^{-1}$ (720 rpm). Again, the differences were small, so important effects
567 are not expected.
568 As Figure 13 shows, an increase in RSF with AFR occurred for some positions of the LFR
569 disc. This trend is very notable for position 3 for CP and is evident, albeit to a much
570 lesser extent, for some other cases, such as position 5 for CP and position 3 for AP. In
571 general, a small increase in RSF can be observed for the different LFR values, but the
572 Tukey test results did not indicate that the increase was statistically significant.
573 These results indicate that a change in the liquid hose position does not greatly alter the
574 homogeneity of the droplet population generated, even though this the homogeneity
575 was slightly lower for the AP. It is a very important finding that the increase in the
576 droplet size is remarkable but the uniformity loss is not. This finding has practical
577 implications for the design of pneumatic sprayers to reduce spray drift in cannon-type
578 spouts. Nevertheless, more research is needed to assess the effect of this variable on
579 spray deposition, coverage, and homogeneity in a real canopy.
580
581 **4. Conclusions**

582 Droplet size and uniformity were measured for two different positions of the liquid hose
583 in the air spout of a pneumatic nozzle in a test bench empirically adjusted to properly
584 simulate a real pneumatic sprayer. Three LFRs and four AFRs were tested, and their
585 influences on droplet size and uniformity were assessed. The following conclusions can
586 be drawn from the study.
587 Changes in the position of the liquid hose inside the air spout significantly increased the
588 droplet size of the generated spray plume, with a mean increase in D50 of 59.45%
589 observed. The spout diameter, liquid flow rate, and air flow rate all produced significant
590 variations in the evaluated droplet size parameters. The spray drift potential can be
591 reduced substantially by changing the liquid hose position from the conventional
592 position to the alternative position. This can reduce spray drift dramatically in
593 applications performed with pneumatic sprayers and thereby contribute to meeting the
594 requirements for the sustainable use of pesticides. The ability to predict the spray
595 droplet size for different combinations of parameters could help farmers increase the
596 safety of their treatments, reduce pollution of the environment, and ensure the
597 sustainability of pneumatic applications in vineyards and compliance with the
598 requirements of the current regulatory framework.
599

600 **Acknowledgements**

601 The authors thank CIMA for the use of their spraying equipment. The first author
602 acknowledges a National Training Program of University Lecturers (FPU) scholarship
603 received from the Spanish Ministry of Education, Culture, and Sport. This work was
604 partially financed by the AgVANCE project (AGL2013-48297-C2-1-R) under the Spanish
605 Ministry of Economy and Competitiveness (MINECO).
606

References

Arvidsson, T., Bergström, L., Kreuger, J., 2011. Spray drift as influenced by meteorological and technical factors. Pest Manag. Sci. 67, 586-598.

Balsari, P., Scienza, A., 2003. Forme di allevamento della vite e modalità di distribuzione dei fitofarmaci. Ed. Informatore Agrario S.p.a., 352.

Balsari, P., Tamagnone, M., Marucco, P., Matta F., 2016. How air liquid perameters affect droplet size: experiences with different pneumatic nozzles. Asp. Appl. Biol.: Int. Adv. Pestic. 132, 265-271.

Baetens, K., Ho, Q.T., Nuyttens, D., Schampheleire, M. de, Endalew, A., Hertog, M., Nicolai, B., Ramon, H., Verboven, P., 2008. Development of a 2-D-diffusion advection model for fast prediction of field drift. Atmos. Environ. 43, 1674-1682.

Benbrook, C.M., Baker, B.P. 2014. Perspective on dietary risk assessment of pesticide residues in organic food. Sustainability 6, 3552–3570.

Bird, S.L., Esterly, D.M., Perry, S.G., 1996. Atmospheric pollutants and trace gases. Off-target deposition of pesticides from agricultural aerial spray applications. J. Environ. Qual. 25, 1095-1104.

Bode, L.E., 1984. Downwind drift deposits by ground applications. In Proceedings Pesticide Drift Management Symposium. 50.

Bode, L.E., Butler, B.J., Goering, C.E., 1976. Spray drift and recovery as affected by spray thickener, nozzle type, and nozzle pressure. Trans. ASAE 19(2), 213-218

627 Bouse, L.F., Kirk, I.W., Bode, L.E., 1990. Effect of spray mixture on droplet size. Trans.
628 ASAE 33(3), 783-788.

629 Butler Ellis, M.C., Lane, A.G., O'Sullivan, C.M., Alanis, R., Harris, A., Stallinga, H., Zande, J.C.
630 van de, 2014. Bystander and resident exposure to spray drift from orchard applications:
631 field measurements, including a comparison of spray drift collectors. Asp. Appl. Biol.: Int.
632 Adv. Pestic. 122, 187-194.

633 Butler Ellis, M.C., Lane, A.G.; O'Sullivan, C.M., Miller, P.C.H., Glass, C.R. 2010. Bystander
634 exposure to pesticide spray drift: New data for model development and validation.
635 Biosyst. Eng. 107, 162–168.

636 Byass JB and Lake JR, 1977. Spray drift from a tractor-powered field sprayer. Pestic. Sci.
637 8: 117–126.

638 Combellack, J.H., 1982. Loss of herbicides from ground sprayers. Weed Res. 22, 193-204.

639 Combellack, J.H., Western, N.M., Richardson, R.G., 1996. A comparison of the drift
640 potential of a novel twin fluid nozzle with conventional low volume flat fan nozzles
641 when using a range of adjuvants. Crop Prot. 15(2), 147-152.

642 Dabrowski, J.M., Schulz, R. 2003. Predicted and measured levels of azinphosmethyl in
643 the Lourens River, South Africa. Comparison of runoff and spray drift. Environ. Toxicol.
644 Chem. 22, 494–500.

645 Davis, B.N.K., Williams, C.T. 1990. Buffer zone widths for honeybees from ground and
646 aerial spraying of insecticides. Environ. Pollut. 63, 247–259.

647 Dekeyser, D., Foqué, D., Duga, A.T., Verboven, P., Hendrickx, N., Nuyttens, D., 2014. Spray
648 deposition assessment using different application techniques in artificial orchard trees.
649 Crop Prot. 64, 187-197.

650 Delele, M.A., Jaeken, P., Debaer, C., Baetens, K., Endalew, A.M., Ramon, H., Nicolaï, B.M.,
651 Verboven, P., 2007. CFD prototyping of an air-assisted orchard sprayer aimed at drift
652 reduction. Comput. Electron. Agric. 55, 16–27.

653 Derksen, R.C., Zhu, H., Fox, R.D., Brazee, R.D., Krause, C.R., 2007. Coverage and drift
654 produced by air induction and conventional hydraulic nozzles used for orchard
655 applications. Trans. ASABE 50, 1493-1501.

656 Di Prinzio, A., Behmer, S., Magdalena, J.C. 2010. Equipos pulverizadores terrestres. In:
657 Tecnología de aplicación de agroquímicos. Argentina: Área de comunicaciones del INTA
658 Alto Valle. cap. 9, 107-120 (In Spanish).

659 Doruchowski, G., Labanowska, B., Goszczynski, W., Godyń, A., Holownicki, R., 2002. Spray
660 deposit, spray loss and biological efficacy of chemicals applied with different spraying
661 techniques in black currants. EJPAU 5(2), #01. Available Online:
662 http://www.ejpau.media.pl/volume5/issue2/engineering/art-01.html

663 Doruchowski, G., Świechowski, W., Masny, S., Maciesiak, A., Tartanus, M., Bryk, H.,
664 Hołownicki, R., 2017. Low-drift nozzles vs. standard nozzles for pesticide application in
665 the biological efficacy trials of pesticides in apple pest and disease control. Sci. Tot. Env.
666 575, 1239-1246.

667 Duga, A.T., Ruysen, K., Dekeyser, D., Nuyttens, D., Bylemans, D., Nicolai, B.M., Verboven,
668 P., 2015. Spray deposition profiles in pome fruit trees: Effects of sprayer design, training
669 system and tree canopy characteristics. Crop Prot. 67, 200-213.

670 Ernst, W.R., Jonah, P.; Doe, K., Julien, G., Hennigar, P. 1991. Toxicity to aquatic organisms
671 of off-target deposition of endosulfan applied by aircraft. Environ. Toxicol. Chem. 10,
672 103–114.

673 European Community, 2009. Directive 2009/128/EC of the European parliament and
674 the council of 21 October 2009 establishing a framework for community action to
675 achieve the sustainable use of pesticides. Official Journal of the European Union L 309,
676 71-86.

677 Felsot, A.S., Unsworth, J.B., Linders, J.B.H.J., Roberts, G. 2011. Agrochemical spray drift;
678 assessment and mitigation—A review. J. Environ. Sci. Health B 46, 1–23.

679 Frost, K.R., Ware, G.W., 1970. Pesticide drift from aerial and ground applications. Agr.
680 Eng. 51 (8), 460-464.

681 Ganzelmeier, H., Rautmann, D., 2000. Drift, drift reducing sprayers and sprayer testing.
682 Asp. Appl. Biol.: Int. Adv. Pestic. 57, 1-10.

683 Gil, E., Balsari, P., Gallart, M., Llorens, J., Marucco, P., Andersen, P.G., Fàbregas, X., Llop, J.
684 2014. Determination of drift potential of different flat fan nozzles on a boom sprayer
685 using a test bench. Crop Protection, 56: 58-68

686 Gil, E., Gallart, M., Balsari, P., Marucco, P., Almajano M.P., Llop, J., 2015. Influence of wind
687 velocity and wind direction on measurements of spray drift potential of boom sprayers
688 using drift test bench. Agric. For. Meteorol. 202, 94-101.

689 Grella, M., Gallart, M., Marucco, P., Balsari, P., Gil, E., 2017. Ground deposition and
690 airborne spray drift assessment in vineyard and orchard: the influence of environmental
691 variables and sprayer settings. Sustainability 9(5), 728.

692 Grover, R., Kerr, L.A., Maybank, J., Yoshidja, K., 1978. Field measurement of droplet drift
693 from ground sprayers. I. Sampling, analytical and data integration techniques. Can. J.
694 Plant Sci. 58(3), 611-622.

695 Guler, H., Zhu, H., Ozkan, H.E., Derksen, R.C., Yu, Y., Krause, C.R., 2007. Spray
696 characteristics and drift reduction potential with air induction and conventional flat fan
697 nozzles. T. ASABE 50(3), 745–754.

698 Hair, J.F., Anderson, R.E., Tatham, R.L., Black, W.C., 1999. Multivariate Data Analysis, 7th
699 edition. ed. Prentice Hall.

700 Hilz, E., Vermeer, A.W.P., 2013. Spray drift review: The extent to which a formulation can
701 contribute to spray drift reduction. Crop Prot. 44, 75–83.

702 Hobson, P.A., Miller, P.C.H., Walklate, P.J., Tuck, C.R., Western, N.M., 1990. Spray drift
703 from hydraulic spray nozzles: The use of a computer simulation model to examine
704 factors influencing drift. In Conference Proceedings AgEng 1990, Berlin. 1-11.

705 Hobson, P.A., Miller, P.C.H., Walklate, P.J., Tuck, C.R., Western, N.M., 1993. Spray drift
706 from hydraulic spray nozzles: the use of a computer simulation model to examine
707 factors influencing drift. J. Agr. Eng. Res. 54, 293-305.

708 Hofman V, Solseng E, 2001. Reducing spray drift. North Dakota State University NDSU
709 Extension Service AE-1210, Fargo, ND.

ISO, 2005. ISO 22866:2005: Equipment for crop protection—Methods for field measurements of spray drift. International Organization for Standardization, Geneva, Switzerland.

Lahr, J., Gadji, B., Dia, D. 2000. Predicted buffer zones to protect temporary pond invertebrates from groundbased insecticide applications against desert locusts. Crop Prot. 19, 489–500.

Llorens, J., Gallart, M., Llop, J., Miranda-Fuentes, A., Gil, E., 2016. Difficulties to apply ISO 22866 requirements for drift measurements. A particular case of traditional olive tree plantations. Asp. Appl. Biol. 132, 31–38.

Manhani, G.G., Teixeira, M.M., Fernandes, H.C., Zolnier, S., Sasaki, R.S., 2013. Developing a system to control the air flow of a pneumatic sprayer. Bioscience Journal. 29, 667–675.

Márquez, L. 2007. Pulverización y pulverizadores neumáticos. Agrotécnica, No. 2, 2007: 34—41 (in Spanish).

Marrs, R.H., Frost, A.J., Plant, R.A., Lunnis, P. 1993. Determination of buffer zones to protect seedlings of non-target plants from the effects of glyphosate spray drift. Agric. Ecosyst. Environ. 45, 283–293.

Miller, P.C.H., Hadfield, D.J., 1989. A simulation model of the spray drift from hydraulic nozzles. J. Agr. Eng. Res. 42, 135-147.

Nuyttens, D., Baetens, K., De Schampheleire, M., Sonck, B., 2007a. Effect of nozzle type, size and pressure on spray droplet characteristics. Biosyst. Eng. 97(3), 333-345.

730 Nuyttens, D., Schampheleire, M. De, Baetens, K., Sonck, B., 2007b. The influence of
731 operator-controlled variables on spray drift from field crop sprayers 50, 1129–1140.

732 Nuyttens, D., De Schampheleire, M., Verboven, P., Sonck, B., 2010. Comparison between
733 indirect and direct spray drift assessment methods. Biosyst. Eng. 105(1), 2-12.

734 Nuyttens, D., De Schampheleire, M., Baetens, K., Brusselman, E., Dekeyser, D., Verboven,
735 P., 2011. Drift from field crop sprayers using an integrated approach: Results of a 5-year
736 study. Trans. ASABE 54(2), 403-408.

737 Rautmann, D., Streloke, M., Winkler, R., 2001. New basic drift values in the authorization
738 procedure for plant protection products. Mitteilungen aus der Biologischen
739 Bundesanstaltd fur Land - und Forstwirtschaft 383, 133-141.

740 Southcombe, E.E.S., Miller, P.C.H., Ganzelmeier, H., Zande, J. Van De, Miralles, A., Hewitt,
741 A.J., 1997. The international (BCPC) spray classification system including a drift
742 potential factor, in: Proceedings of the Brighton Crop Protection Conference - Weeds. pp.
743 371–380.

744 Take, M.E., Barry, J.W., Richardson, B. 1996. An FSCBG sensitivity study for decision
745 support systems, Paper No. 961037, ASAE Annual Meeting: Phoenix, AZ.

746 TOPPS-Prowadis Project. 2014. Best management practices to reduce spray drift.
747 Available online at: http://www.topps-life.org/. Accessed on January 2017.

748 van de Zande, J.C., Holterman, H.J., Wenneker, M., 2008. Nozzle classification for drift
749 reduction in orchard spraying: Identification of drift reduction class threshold nozzles.
750 Agric. Eng. Int. CIGR Ejournal X, 1–12.

751 Van den Berg, F., Kubiak, R., Benjey, W.G., Majewski, M.S., Yates, S.R., Reeves, G.L., Smelt,
752 J.H., Linden, A.M.A.V.D. 1999. Emission of pesticides into the air. Water Air Soil Pollut.
753 115, 195–218.

754 Yates, W.E., Cowden, R.E., Akesson, N.B., 1985. Drop size spectra from nozzles in high-
755 speed airstream. Trans. ASAE 28(2), 405-410.

756 Zhu, H., Reichard, D.L., Fox, R.D., Brazee, R.D., Ozkan, H.E., 1994. Simulation of drift of
757 discrete sizes of water droplets from field sprayers. Trans. ASAE 37(5), 1401-1407.

758

759

760

761 Table 1. Studied variables with adjustable parameters and selected levels for each one.
762

Studied parameter	**Air spout diameter** (SD)	**Liquid flow rate** (LFR)	**Air flow rate** (AFR)
Studied levels	50/70 mm	1.00/1.64/2.67 L min^{-1}	0.280/0.312/0.348/0.376 m^3 s^{-1}
Regulation based on	Position of the liquid hose	Position of the regulatory disc	Rotary speed of the fan
Positions tested	Conventional/Alternative	Positions 3/5/7	541/598/663/720 rpm

763

764

765 Table 2. Results of the adjustment of the rotary speed values to make the pressure match in both systems.
766

Parameter		Values			
Sprayer rotary speed	(rpm)	350	400	450	500
Measured pressure	(mm_{H_2O})	180	240	300	380
Calculated prototype speed	(rpm)	462	552	642	732
Adjusted prototype speed	(rpm)	541	598	663	720

767
768

769

770 Table 3. Mean air speeds for sampling positions 0, 5, and 10 along the longitudinal axis of the air spout and absolute and relative air speed drops.
771

	Air speed (m s^{-1})				
Prototype	Sampling position			Δspeed	Δspeed
rpm	0	5	10	(m s^{-1})	(%)
350	51.80	46.51	46.84	4.23	8.29
400	58.83	53.44	53.85	4.98	8.47
450	65.90	60.54	60.30	5.60	8.50
500	74.10	67.16	67.75	6.35	8.57
541	79.51	72.39	72.76	6.74	8.48
550	81.36	73.81	74.36	6.99	8.60
600	88.58	80.69	81.02	7.56	8.53
650	96.31	87.68	88.56	7.75	8.04
663	97.70	89.26	89.60	8.11	8.30
700	103.78	94.92	95.76	8.02	7.73
				Mean	8.35
				SD	0.28
				CV (%)	3.31

772

773 **Figure captions**

774 Figure 1. Laboratory setup for the test bench and difference spaces: A. Spraying
775 equipment, B. Spray droplet measurement instruments, and C. Trial control and data
776 acquisition elements.
777 Figure 2. Spraying circuit used in the test bench.
778 Figure 3. Conventional (CP) and alternative (AP) positions of insertion of the liquid hose
779 in the air spout.
780 Figure 4. Air pressure sampling position in: a) the real sprayer, and b) the prototype.
781 Figure 5. Implement for measuring the air speed in the centre of the air spout.
782 Figure 6. Malvern SprayTec® droplet size analyser in the laboratory set-up.
783 Figure 7. Air pressure versus rotary speed for the sprayer and the test bench.
784 Figure 8. Air speed values along the longitudinal axis of the air spout.
785 Figure 9. Boxplots for the variables D50 (a), D10 (b), D90 (c), V100 (d), and RSF (e). The
786 boxplots include all of the combinations of AFR and LFR considered.
787 Figure 10. D50 values for different combinations of variables for the two positions of the
788 liquid hose. The error bars indicate the standard errors.
789 Figure 11. Mean relative differences in D50 between the two liquid hose positions for
790 every combination of AFR and LFR.
791 Figure 12. V_{100} for different combinations of variables for the two positions of the liquid
792 hose. The error bars indicate the standard errors.
793 Figure 13. Mean relative SPAN factor (RSF) for every tested combination of LFR and AFR
794 for the two tested positions of the liquid hose. The error bars indicate the standard
795 errors.

Figures in order

Click here to download Figure: FIGURES without text.pptx

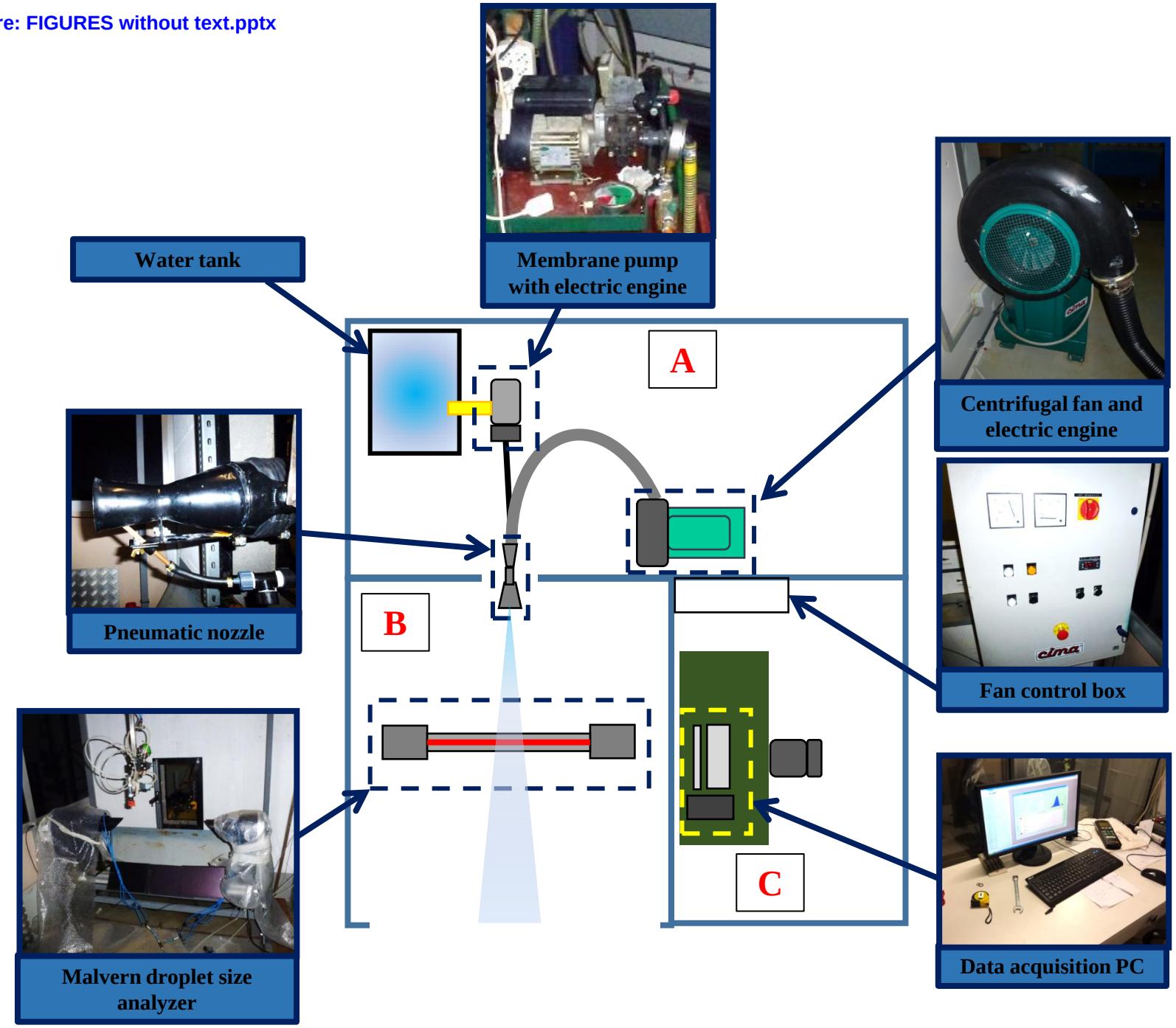

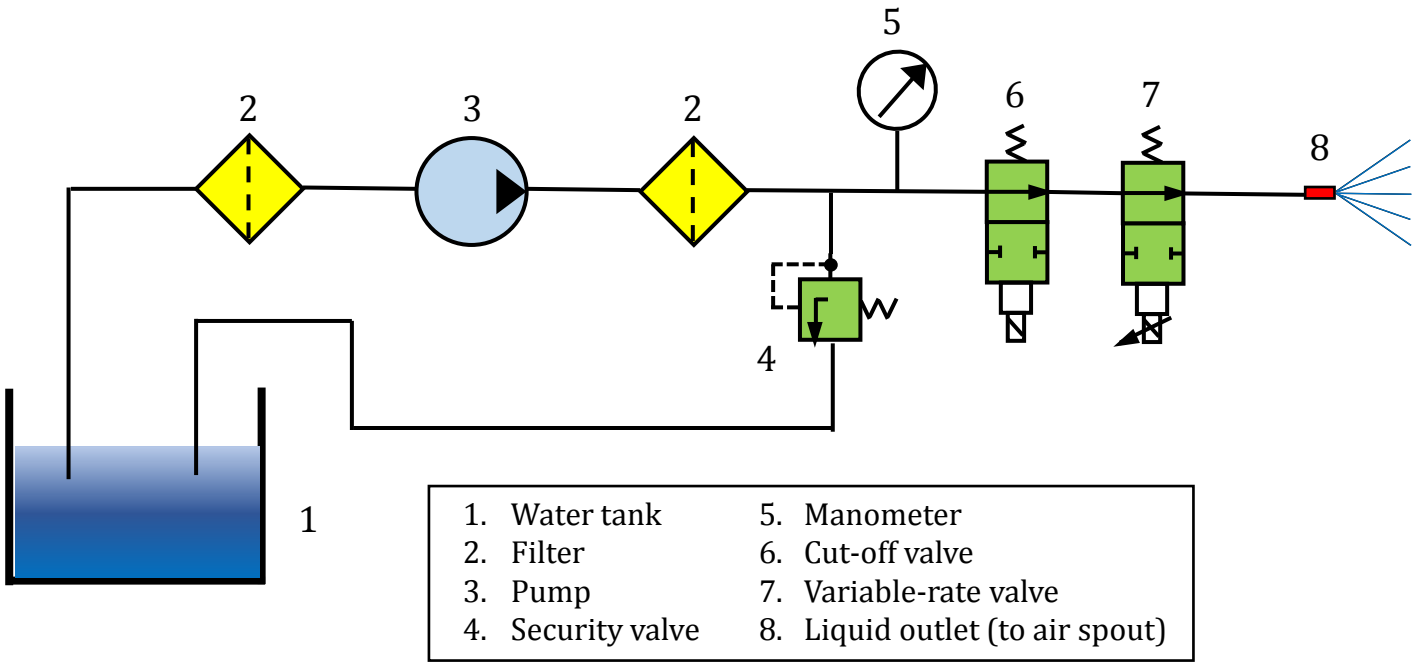

1. Water tank
2. Filter
3. Pump
4. Security valve
5. Manometer
6. Cut-off valve
7. Variable-rate valve
8. Liquid outlet (to air spout)

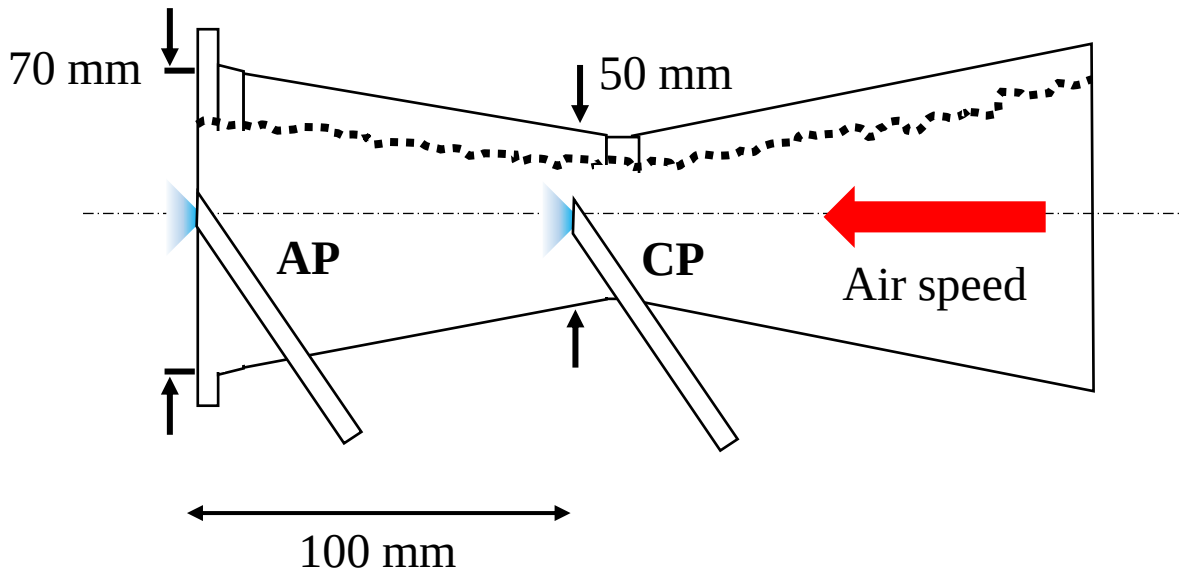
70 mm
50 mm
AP
CP
Air speed
100 mm

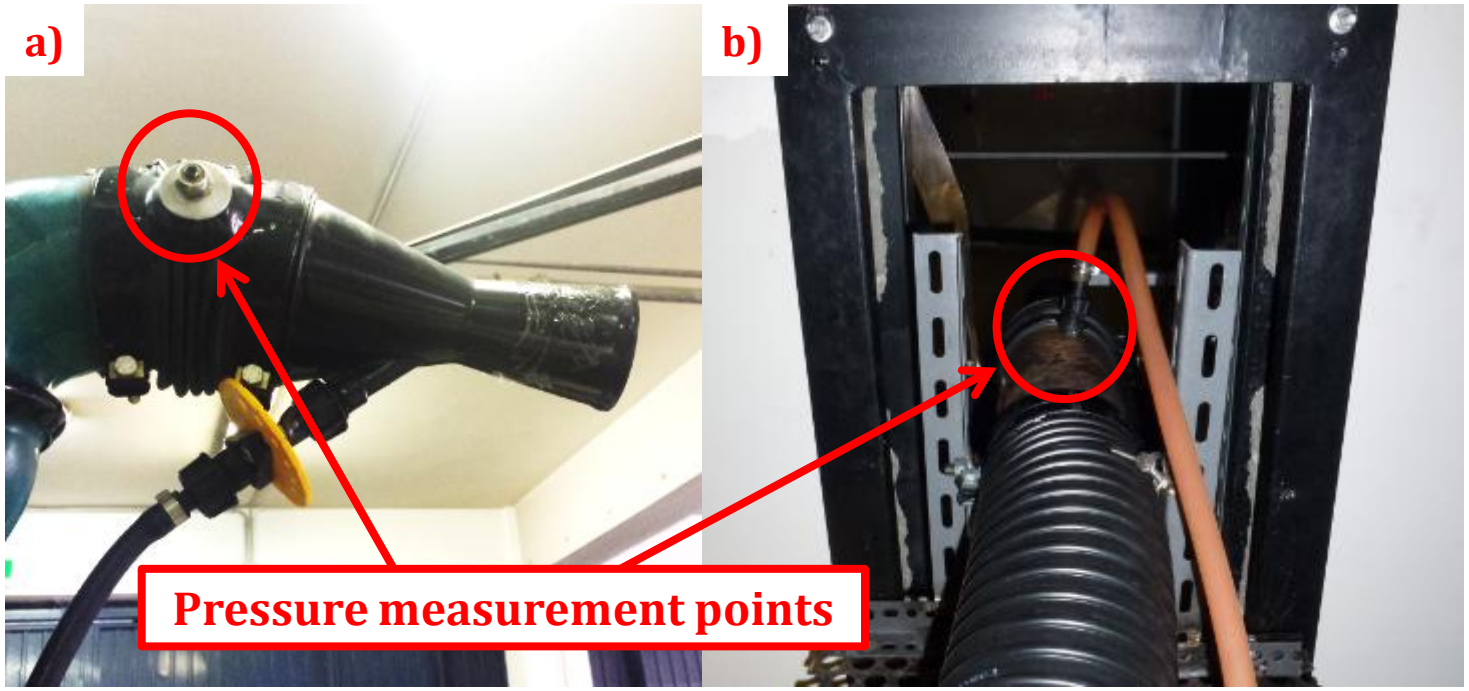
a)
b)
Pressure measurement points


CIMA 18/120

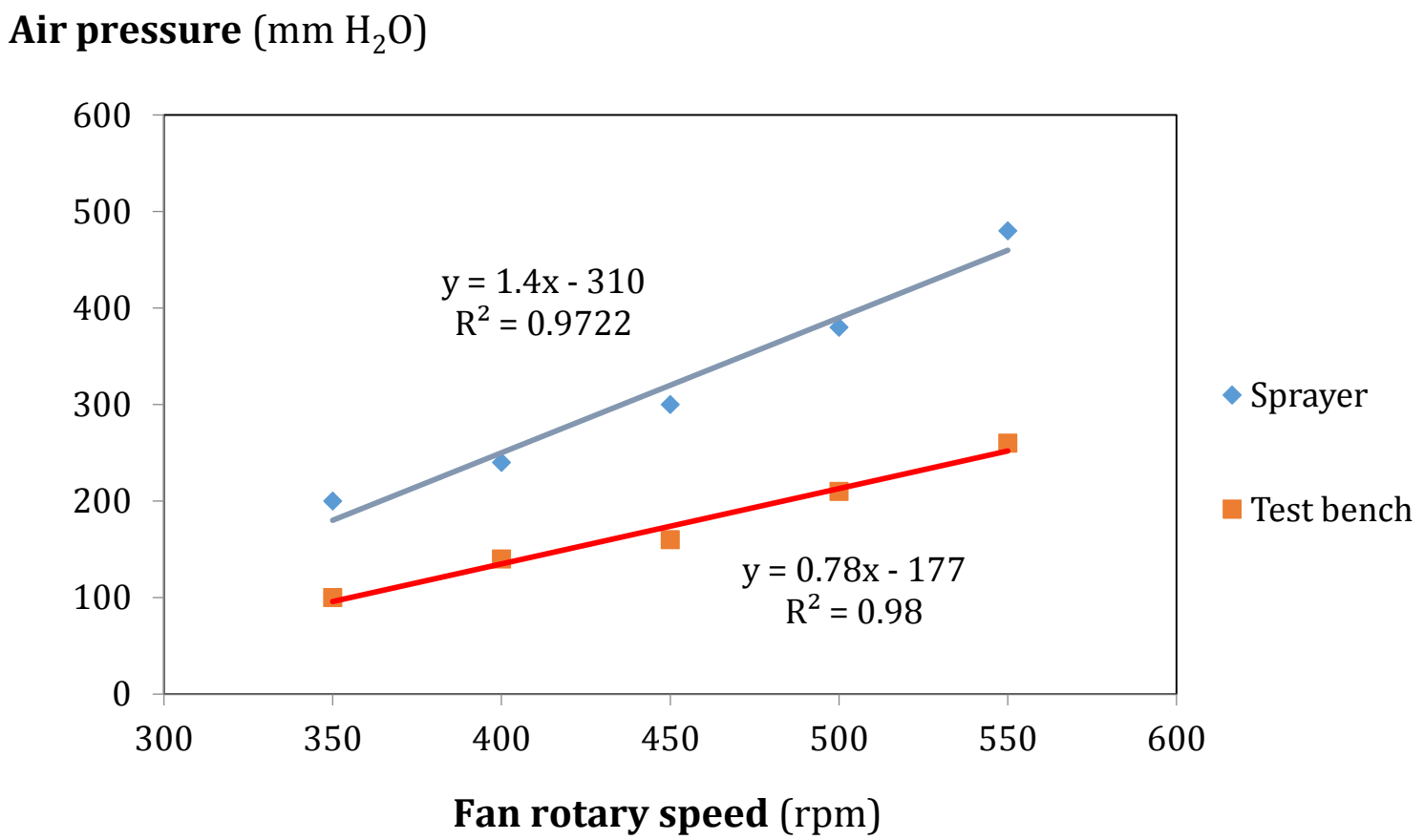
Air pressure (mm H2O)
600
500
400
300
200
100
0
y = 1.4x - 310
R² = 0.9722
y = 0.78x - 177
R² = 0.98
Sprayer
Test bench
300
350
400
450
500
550
600
Fan rotary speed (rpm)

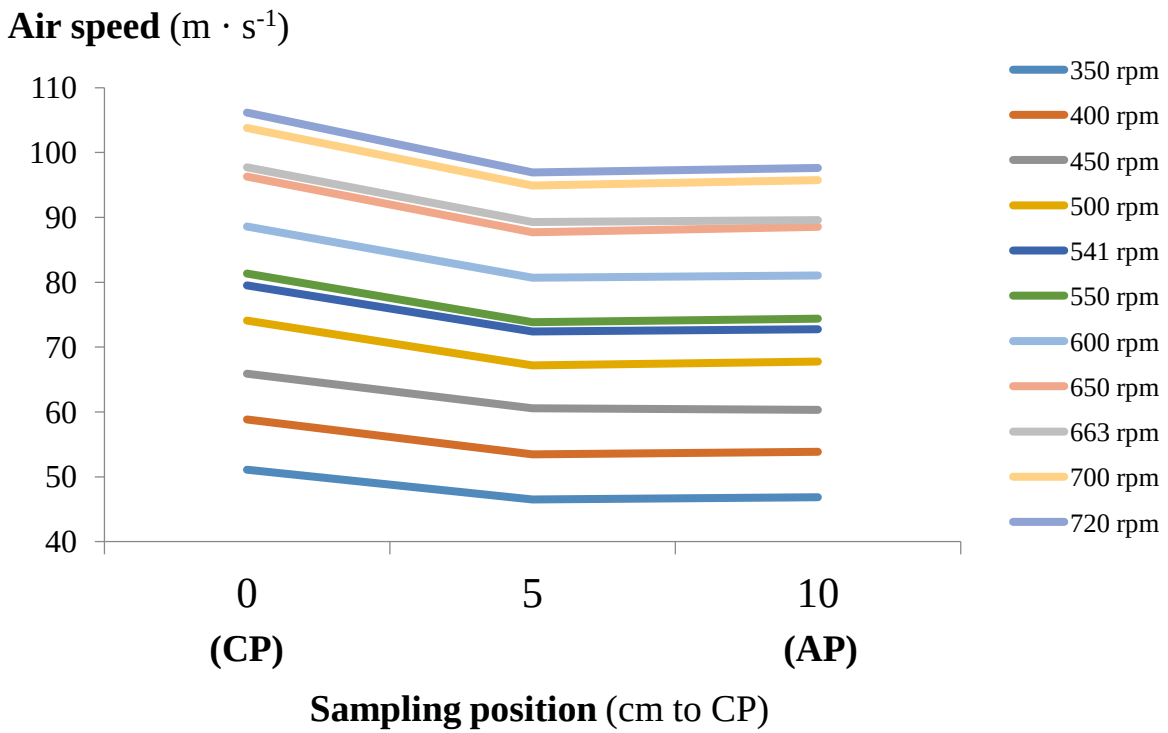
Air speed (m · s-1)
110
100
90
80
70
60
50
40
0
5
10
(CP)
(AP)
Sampling position (cm to CP)
350 rpm
400 rpm
450 rpm
500 rpm
541 rpm
550 rpm
600 rpm
650 rpm
663 rpm
700 rpm
720 rpm

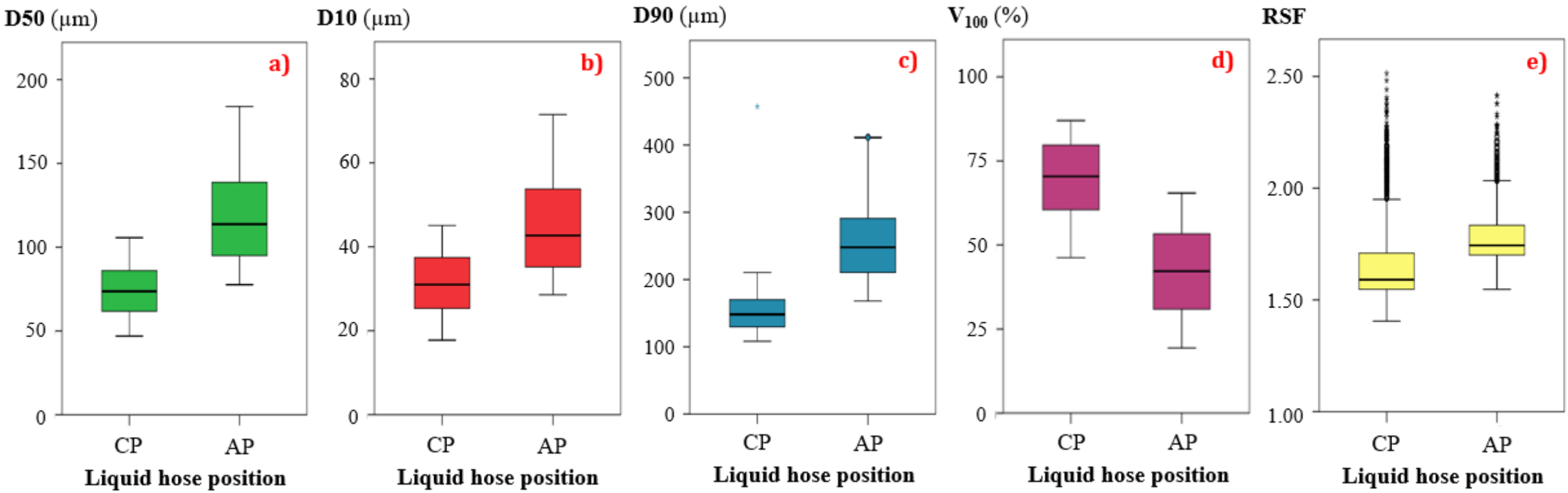
D50 (µm)
a)
200
150
100
50
0
CP
AP
Liquid hose position
D10 (µm)
b)
80
60
40
20
0
CP
AP
Liquid hose position
D90 (µm)
c)
500
400
300
200
100
0
CP
AP
Liquid hose position
V100 (%)
d)
100
75
50
25
0
CP
AP
Liquid hose position
RSF
e)
2.50
2.00
1.50
1.00
CP
AP
Liquid hose position

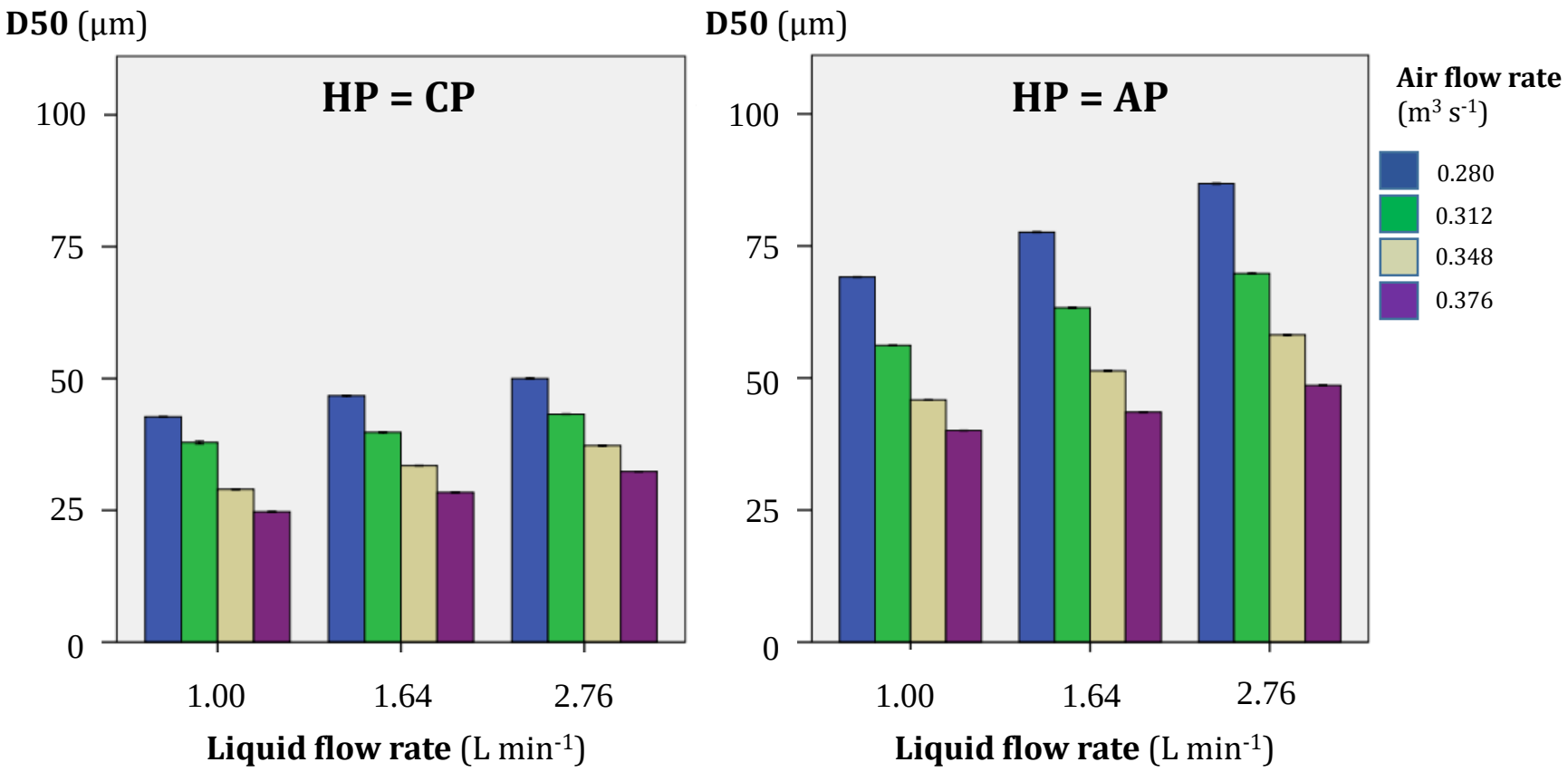
D50 (µm)
HP = CP
100
75
50
25
0
1.00
1.64
2.76
Liquid flow rate (L min-1)
D50 (µm)
HP = AP
100
75
50
25
0
1.00
1.64
2.76
Liquid flow rate (L min-1)
Air flow rate
(m3 s-1)
0.280
0.312
0.348
0.376

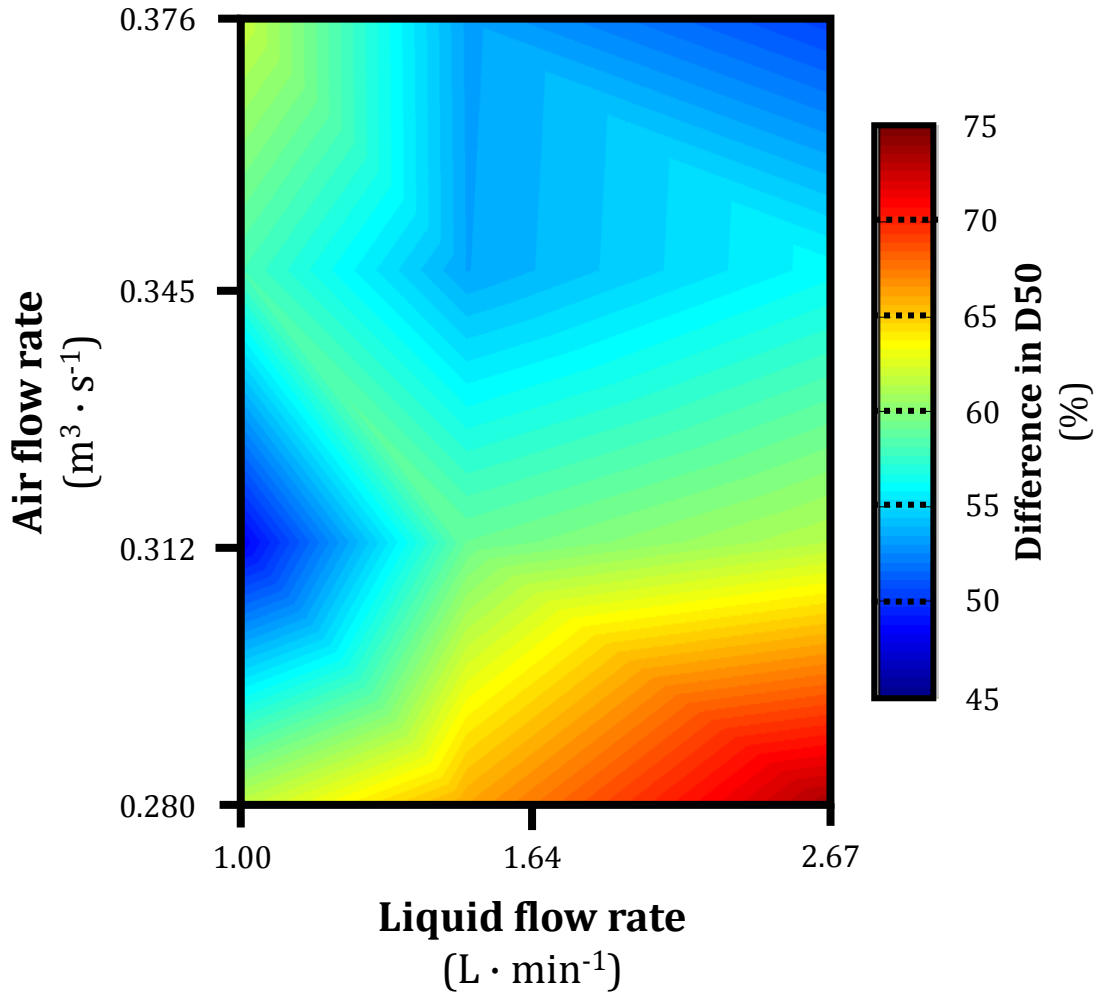
0.376
0.345
0.312
0.280
Air flow rate
(m³ · s⁻¹)
1.00
1.64
2.67
Liquid flow rate
(L · min⁻¹)
75
70
65
60
55
50
45
Difference in D50
(%)

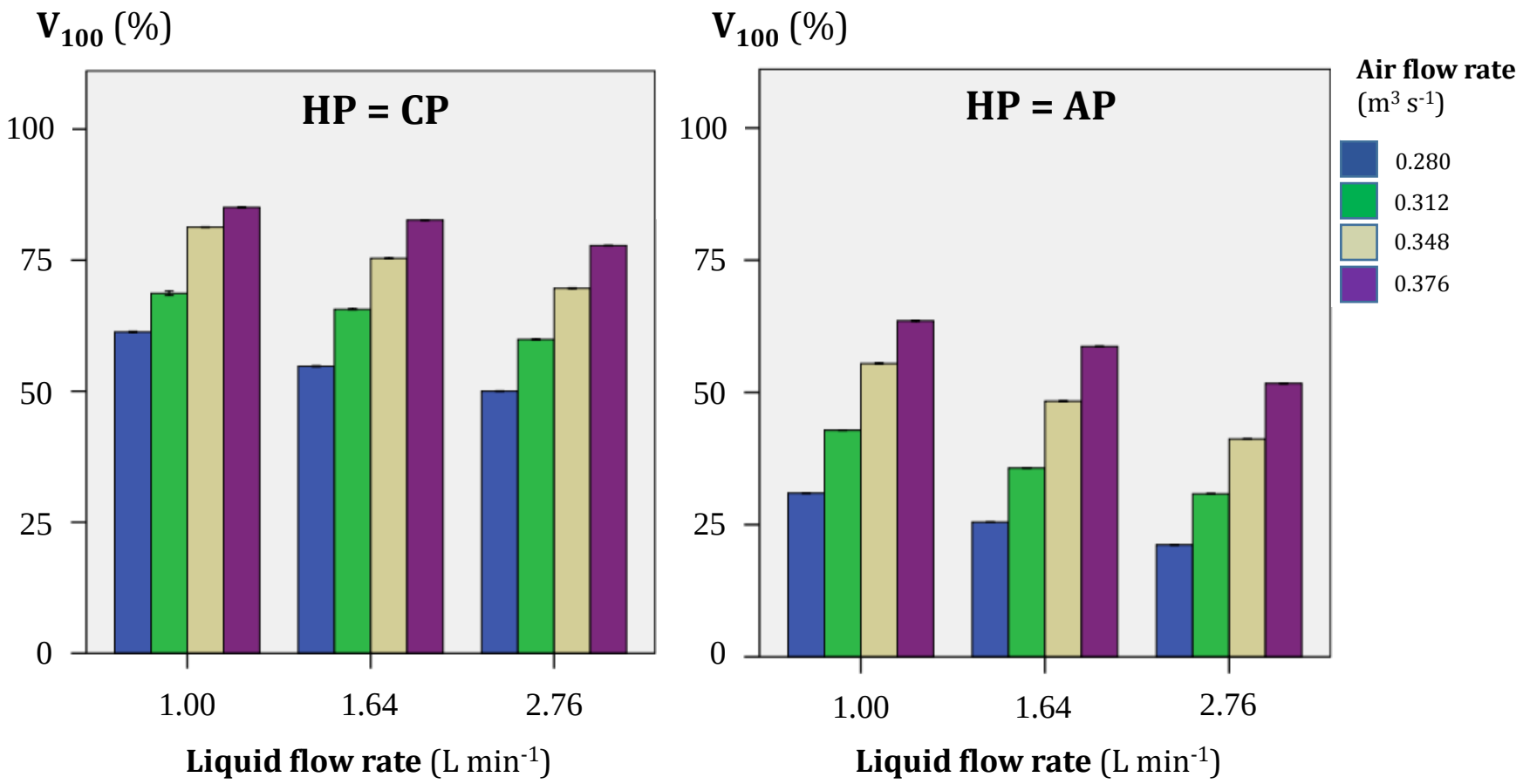
V_{100} (%)
HP = CP
100
75
50
25
0
1.00
1.64
2.76
Liquid flow rate (L min-1)
V_{100} (%)
HP = AP
100
75
50
25
0
1.00
1.64
2.76
Liquid flow rate (L min-1)
Air flow rate
(m3 s-1)
0.280
0.312
0.348
0.376

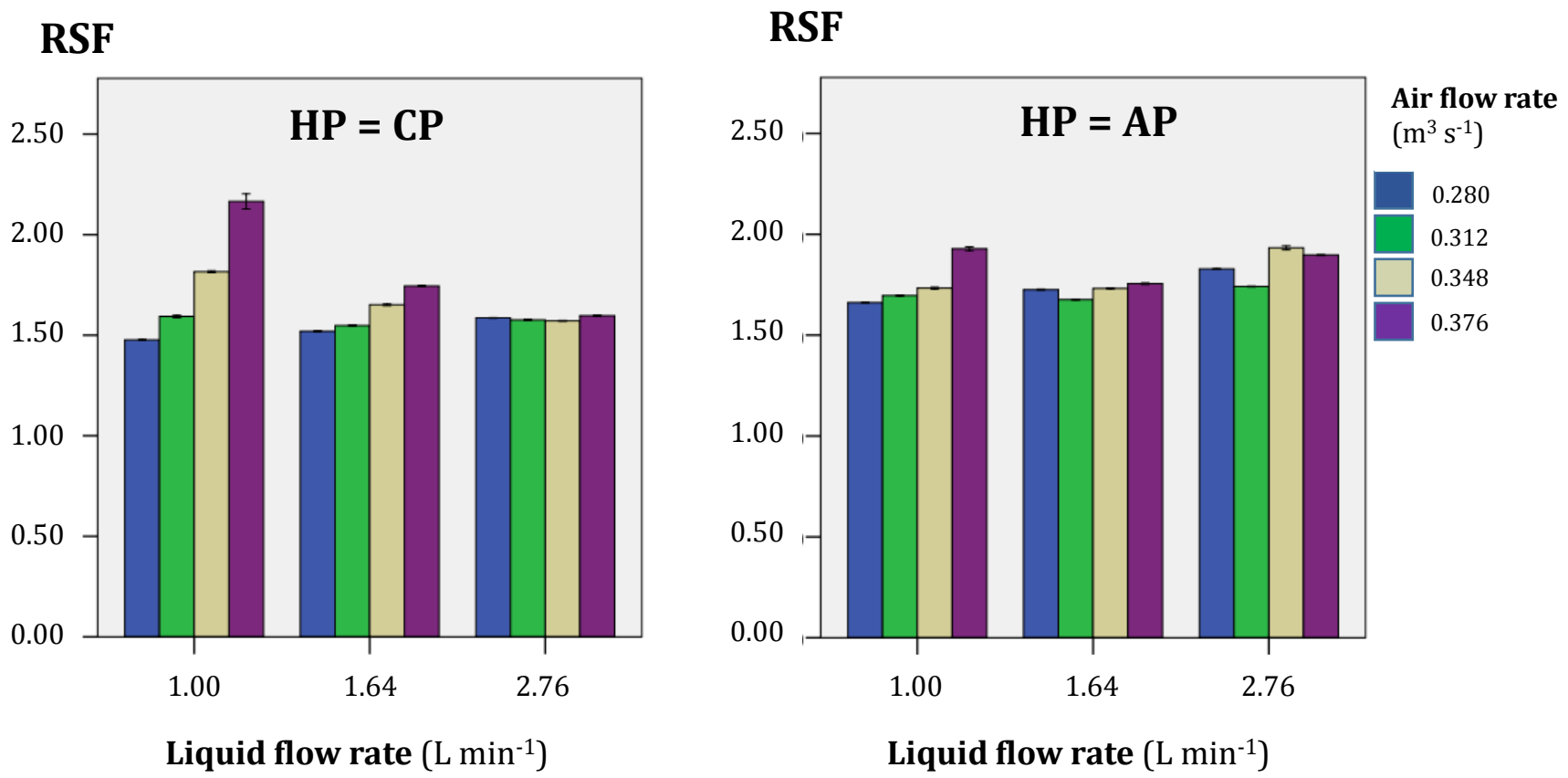
RSF
HP = CP
2.50
2.00
1.50
1.00
0.50
0.00
1.00
1.64
2.76
Liquid flow rate (L min-1)
RSF
HP = AP
2.50
2.00
1.50
1.00
0.50
0.00
1.00
1.64
2.76
Liquid flow rate (L min-1)
Air flow rate
(m3 s-1)
0.280
0.312
0.348
0.376